

# SIMULTANEOUS IDENTIFICATION AND DENOISING OF DYNAMICAL SYSTEMS\*

JEFFREY M. HOKANSON<sup>†</sup>, GIANLUCA IACCARINO<sup>‡</sup>, AND ALIREZA DOOSTAN<sup>†</sup>

**Abstract.** In recent years there has been a push to discover the governing equations dynamical systems directly from measurements of the state, often motivated by systems that are too complex to directly model. Although there has been substantial work put into such a discovery, doing so in the case of large noise has proved challenging. Here we develop an algorithm for the Simultaneous Identification and Denoising of a Dynamical System (SIDDS). We infer the noise in the state measurements by requiring that the denoised state satisfies the dynamical system with an equality constraint. This contrasts to existing work where the mismatch in the dynamics is added as a penalty in the objective. Assuming the nonlinear differential equation is represented in a pre-defined basis, we develop sequential quadratic programming approach to solve the SIDDS problem featuring a direct solution of KKT system with a specialized preconditioner. We also show how to add a sparsity promotion regularization into SIDDS using an iteratively reweighted least squares approach. Our resulting algorithm obtains estimates of the dynamical system that achieve the Cramér-Rao lower bound up to discretization error. This enables SIDDS to provide substantial improvements compared to existing techniques: SIDDS substantially decreases the data burden for accurate identification, recovers optimal estimates with lower sample rates, and the sparsity promoting variant discovers the correct sparsity pattern with larger noise.

**Key words.** dynamical systems, model discovery, inverse problems, parameter estimation, sparse recovery

**AMS subject classifications.** 34A55, 65L09, 90C55, 93B30

**DOI.**

**1. Introduction.** We consider the problem of identifying a dynamical system from measurements of its state. Suppose the state of this system  $\mathbf{x} \in \mathbb{R}^d$  satisfies a first order, autonomous ordinary differential equation (ODE)

$$(1.1) \quad \begin{cases} \dot{\mathbf{x}}(t) = \mathbf{f}(\mathbf{x}(t)), \\ \mathbf{x}(0) = \mathbf{x}_0, \end{cases} \quad \text{where } \mathbf{f} : \mathbb{R}^d \rightarrow \mathbb{R}^d.$$

Our goal is to identify  $\mathbf{f}$  given access to  $m$  noisy observations of the state  $\{\mathbf{y}_j\}_{j=1}^m$ , where  $\mathbf{y}_j \approx \mathbf{x}(t_j)$  at times  $\{t_j\}_{j=1}^m \subset [0, T]$ . This problem emerges in a variety of contexts from model reduction [26] to system identification [6].

**1.1. Parameterization.** An important choice for recovering the operator  $\mathbf{f}$  is its parameterization. Here, we express  $\mathbf{f}$  as a sum of  $n$  scalar-valued basis functions  $\phi_k : \mathbb{R}^d \rightarrow \mathbb{R}$  with corresponding coefficients  $\mathbf{c}_k \in \mathbb{R}^d$  following [6]

$$(1.2) \quad \mathbf{f}(\mathbf{x}; \mathbf{C}) := \sum_{k=1}^n \mathbf{c}_k \phi_k(\mathbf{x}), \quad \text{where } \mathbf{C} := \begin{bmatrix} \mathbf{c}_1^\top \\ \vdots \\ \mathbf{c}_n^\top \end{bmatrix} \in \mathbb{R}^{n \times d}.$$

---

\*Submitted to the editors DATE.

**Funding:** This material is based upon work supported by the Department of Energy, National Nuclear Security Administration under Award Number DE-NA0003968.

<sup>†</sup> Department of Aerospace Engineering Sciences, University of Colorado at Boulder, Boulder, CO 80309 (jeffrey@hokanson.us, alireza.doostan@colorado.edu)

<sup>‡</sup> Center for Turbulence Research, Stanford University, Stanford, CA 94305 (jops@stanford.edu)

A typical choice for  $\{\phi_k\}_{k=1}^n$  is a polynomial basis; e.g., total degree-2 basis in two dimensions ( $d = 2$ ) is:

$$\phi_1(\mathbf{x}) = 1, \quad \phi_2(\mathbf{x}) = x_1, \quad \phi_3(\mathbf{x}) = x_2, \quad \phi_4(\mathbf{x}) = x_1^2, \quad \phi_5(\mathbf{x}) = x_1x_2, \quad \phi_6(\mathbf{x}) = x_2^2.$$

Non-polynomial terms such as  $\phi_k(\mathbf{x}) = \sin(x_1)$  can also be incorporated. In some cases, we will further seek a parsimonious, interpretable expression for  $\mathbf{f}$  by seeking a sparse coefficient matrix  $\mathbf{C}$ . There are other parameterizations possible for  $\mathbf{f}$ , for example, a neural network [27].

**1.2. A Naive Least Squares Approach.** A variety of methods exploit a simple linear relationship to estimate the coefficients  $\mathbf{C}$ . Suppose we have access to exact measurements of the state  $\mathbf{x}(t_j)$  and its derivative  $\dot{\mathbf{x}}(t_j)$  and stack these into matrices

$$(1.3) \quad \mathbf{X} := \begin{bmatrix} \mathbf{x}(t_1)^\top \\ \vdots \\ \mathbf{x}(t_m)^\top \end{bmatrix} \in \mathbb{R}^{m \times d} \quad \text{and} \quad \dot{\mathbf{X}} := \begin{bmatrix} \dot{\mathbf{x}}(t_1)^\top \\ \vdots \\ \dot{\mathbf{x}}(t_m)^\top \end{bmatrix} \in \mathbb{R}^{m \times d}.$$

Further, we build the matrix-valued function  $\Phi : \mathbb{R}^{m \times d} \rightarrow \mathbb{R}^{m \times n}$  containing the evaluations of the basis functions:

$$(1.4) \quad \Phi(\mathbf{X}) := \begin{bmatrix} \phi_1(\mathbf{x}(t_1)) & \cdots & \phi_n(\mathbf{x}(t_1)) \\ \vdots & & \vdots \\ \phi_1(\mathbf{x}(t_m)) & \cdots & \phi_n(\mathbf{x}(t_m)) \end{bmatrix} \in \mathbb{R}^{m \times n}.$$

With this notation, based on the differential equation (1.1) and the expansion in (1.2), the coefficients  $\mathbf{C}$  must satisfy the linear system:

$$(1.5) \quad \dot{\mathbf{X}} = \begin{bmatrix} \dot{\mathbf{x}}(t_1)^\top \\ \vdots \\ \dot{\mathbf{x}}(t_m)^\top \end{bmatrix} = \begin{bmatrix} \mathbf{f}(\mathbf{x}(t_1))^\top \\ \vdots \\ \mathbf{f}(\mathbf{x}(t_m))^\top \end{bmatrix} = \begin{bmatrix} \sum_{k=1}^n \mathbf{c}_k^\top \phi_k(\mathbf{x}(t_1)) \\ \vdots \\ \sum_{k=1}^n \mathbf{c}_k^\top \phi_k(\mathbf{x}(t_m)) \end{bmatrix} = \Phi(\mathbf{X})\mathbf{C}.$$

When this problem is well-posed, there is a unique solution for  $\mathbf{C}$  given  $\dot{\mathbf{X}}$  and  $\Phi(\mathbf{X})$ ; numerically,  $\mathbf{C}$  can be identified by solving the least squares problem

$$(1.6) \quad \min_{\mathbf{C} \in \mathbb{R}^{n \times d}} \|\dot{\mathbf{X}} - \Phi(\mathbf{X})\mathbf{C}\|_{\text{F}}^2,$$

where  $\|\cdot\|_{\text{F}}$  denotes the Frobenius norm. However, this problem may not have a unique solution; for example, if there is a linear combination of basis functions encoding a conservation law for the system, then  $\Phi(\mathbf{X})$  will have a nontrivial nullspace.

The limitations of experimental measurements present two difficulties: we may not have access to the derivative  $\dot{\mathbf{x}}(t_j)$  and our measurements  $\mathbf{y}_j$  of  $\mathbf{x}(t_j)$  are invariably contaminated by noise. We can correct the former difficulty by estimating the derivative using finite-difference approximations based on measurements  $\mathbf{y}_j$ . When measurements are uniformly spaced in time with time-step  $\delta$ , e.g.,  $t_j = \delta(j-1)$ , we can build a finite difference matrix  $\mathbf{D} \in \mathbb{R}^{m \times m}$  using a  $q$ -point central difference rule in the interior and an order  $q-1$  accurate rule on the boundary. For example, a



Although we have introduced SIDDS using a similar framework to LSOI, SIDDS can alternatively be derived from a more traditional inverse problem approach; see, e.g. [17]. SIDDS approximately solves the ODE-constrained optimization problem,

$$(1.11) \quad \min_{\mathbf{C} \in \mathbb{R}^{n \times d}, \mathbf{z}_0 \in \mathbb{R}^d, \zeta: [0, T] \rightarrow \mathbb{R}^d} \sum_{j=1}^m \|\mathbf{y}_j - \zeta(t_j)\|_2^2$$

s.t.  $\dot{\zeta}(t) = \mathbf{f}(\zeta(t); \mathbf{C}), \quad \zeta(0) = \mathbf{z}_0.$

In particular, SIDDS (1.10) uses the *discretize-then-optimize* approach to discretize (1.11) in time and uses a *full-space* optimization approach where both the coefficients  $\mathbf{C}$  and predicted state history  $\mathbf{z}_j = \zeta(t_j)$  are variables in the optimization problem; see, e.g. [16]. The full-space approach contrasts to a *reduced-space* approach where the predicted state history  $\mathbf{z}_j$  is implicitly defined by  $\mathbf{C}$  and  $\mathbf{z}_0$ ; i.e., solving

$$(1.12) \quad \min_{\mathbf{C} \in \mathbb{R}^{n \times d}, \mathbf{z}_0 \in \mathbb{R}^d} \sum_{j=1}^m \|\mathbf{y}_j - \zeta(t_j; \mathbf{C}, \mathbf{z}_0)\|_2^2, \quad \text{where} \quad \begin{cases} \dot{\zeta}(t; \mathbf{C}, \mathbf{z}_0) = \mathbf{f}(\zeta(t); \mathbf{C}), \\ \zeta(0; \mathbf{C}, \mathbf{z}_0) = \mathbf{z}_0. \end{cases}$$

The reduced-space problem is then solved using an unconstrained optimization algorithm without storing the state history  $\{\mathbf{z}_j\}_{j=1}^m$  [18, Alg. 2.2.]. Although inexpensive, this approach can yield a hypersensitive objective since when approximating a chaotic system, small changes in  $\mathbf{C}$  and  $\mathbf{z}_0$  yield exponentially increasing changes in  $\zeta(t; \mathbf{C}, \mathbf{z}_0)$  with  $t$ . This, in turn, implies that local information, such as gradients and Hessians, are not accurate beyond some small neighborhood and makes finding a meaningful descent direction challenging. In contrast, our full-space approach has a convex objective and although the equality constraint needs to be satisfied at termination, intermediate iterations do not need to satisfy the constraint exactly allowing more effective exploration of the parameter space.

The SIDDS problem shares similarities with problems in data assimilation [2]. Like data assimilation, we seek to estimate the true state from noisy measurements, and as in some formulations, we seek to estimate the parameters of the underlying differential equation. Unlike SIDDS which is solved using a full space method, most data assimilation algorithms use a reduced space approach due to scaling concerns.

**1.4. A First Example.** Why use SIDDS instead of the existing approaches based on LSOI? In short, SIDDS recovers far more accurate dynamical systems from noisy measurements. As a first example, consider the simple harmonic oscillator  $\ddot{x}(t) = -x(t)$  in first order form:

$$(1.13) \quad \begin{bmatrix} \dot{x}_1 \\ \dot{x}_2 \end{bmatrix} = \begin{bmatrix} 0 & 1 \\ -1 & 0 \end{bmatrix} \begin{bmatrix} x_1 \\ x_2 \end{bmatrix} \quad \text{with} \quad \begin{bmatrix} x_1(0) \\ x_2(0) \end{bmatrix} = \begin{bmatrix} 1 \\ 0 \end{bmatrix}.$$

Reconstructing this system, we use two linear basis functions:  $\phi_1(\mathbf{x}) = x_1$  and  $\phi_2(\mathbf{x}) = x_2$ . Then if we take  $m = 2000$  measurements with sample rate  $\delta = 10^{-2}$  that are contaminated with i.i.d. standard normal noise with unit covariance, using the 3-point derivative approximation in (1.7), we recover the systems

LSOI	SIDDS
$\begin{bmatrix} \dot{x}_1 \\ \dot{x}_2 \end{bmatrix} = \begin{bmatrix} -0.23580696 & 2.85537791 \\ -2.60758784 & 0.2062968 \end{bmatrix} \begin{bmatrix} x_1 \\ x_2 \end{bmatrix}$	$\begin{bmatrix} \dot{x}_1 \\ \dot{x}_2 \end{bmatrix} = \begin{bmatrix} -0.01155883 & 0.99851078 \\ -1.0097105 & -0.0019787 \end{bmatrix} \begin{bmatrix} x_1 \\ x_2 \end{bmatrix}$

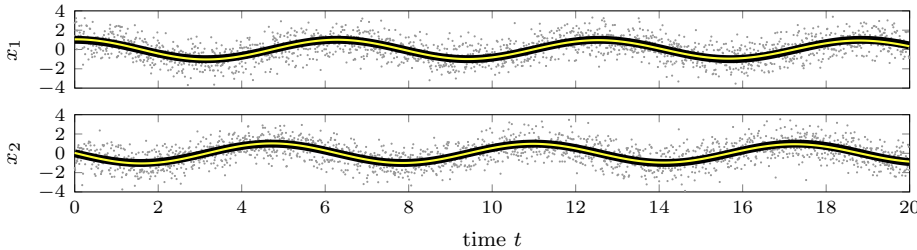


FIG. 1.1. *SIDDS* accurately denoises the state and recovers the dynamical system in the simple harmonic oscillator example. Here the true system evolution is shown as a black line, the measured data as gray points, and the recovered system as a yellow line.

Here *SIDDS*'s estimate is accurate to 2-significant figures; *LSOI* captures none!

The reason why *SIDDS* performs so much better than *LSOI* is that, subject to optimization algorithm finding the global minimizer,  $\mathbf{Z}$  is a maximum likelihood estimate of the true data  $\mathbf{X}$  so that  $\mathbf{Z} \approx \mathbf{X}$  as illustrated in Figure 1.1. With this accurate estimate of  $\mathbf{X}$  in  $\mathbf{Z}$ , *SIDDS* provides an accurate estimate of the coefficients  $\mathbf{C}$ . In contrast, *LSOI* does not provide a maximum likelihood estimate of  $\mathbf{C}$  due to the way it correlates noise in the expression  $\mathbf{D}\mathbf{Y} - \Phi(\mathbf{Y})\mathbf{C}$ . Details concerning these results are provided in section 3.

**1.5. Sparsity Promotion.** With an eye to obtain an easily interpretable expansion of  $\mathbf{f}$  in the basis  $\{\phi_k\}_{k=1}^n$  as in (1.2), it is common to apply a regularization to encourage the coefficients  $\mathbf{C}$  to be sparse. *Sparse Identification of Nonlinear Dynamics* (*SINDy*) encompasses a variety of algorithms using different techniques to promote sparsity in  $\mathbf{C}$ , many inspired by compressed sensing. For example, *Sequentially Thresholded Least Squares* (*STLS*) (see, e.g., [5]) can be used iteratively to remove small coefficients in  $\mathbf{C}$  [6]. Another approach is to add an  $\ell_p$ -norm regularization term to the objective, i.e.,

$$(1.14) \quad \min_{\mathbf{C}} \|\mathbf{D}\mathbf{Y} - \Phi(\mathbf{Y})\mathbf{C}\|_{\mathbb{F}}^2 + \lambda R_p(\text{vec}(\mathbf{C})) \quad \text{where} \quad R_p(\mathbf{w}) := \begin{cases} \|\mathbf{w}\|_p^p, & p > 0; \\ \|\mathbf{w}\|_0, & p = 0; \end{cases}$$

where  $\text{vec}(\cdot)$  denotes row-major vectorization and  $\|\mathbf{w}\|_0$  is the number of nonzero entries in  $\mathbf{w}$ . This is a nonconvex problem for  $p < 1$  and nondifferentiable for  $p = 0$ ; however, in many applications small values of  $p$ , especially  $p = 0$ , provide better recovery. There are a variety of techniques that can be used to solve (1.14), such as *Iteratively Reweighted Least Squares* (*IRLS*) [4, Subsec. 4.5.2] or *Iteratively Reweighted  $\ell_1$ -norm* (*IR $\ell_1$* ) [7]. The latter is used for recovering dynamical systems in [9] with an accuracy better than that of *STLS*. Our approach with *SIDDS* will be to promote sparsity by adding a similar regularization penalty

$$(1.15) \quad \begin{aligned} & \min_{\mathbf{C}, \mathbf{Z}} \|\mathbf{Y} - \mathbf{Z}\|_{\mathbb{F}}^2 + \alpha R_p(\text{vec}(\mathbf{C})) \\ & \text{s.t. } \mathbf{D}\mathbf{Z} = \Phi(\mathbf{Z})\mathbf{C}. \end{aligned}$$

We refer to this variant as *SIDDS*+ $\ell_p$ . In our numerical experiments, we choose  $p = 0$  and use regularized *IRLS* [8] to provide a quadratic approximation of  $R_p$ .

Although these sparsity promoting techniques will often regularize the problem and reduce the impact of noise, simply identifying the correct sparsity structure is not

sufficient to obtain an accurate parameter estimate when using the LSOI objective. Returning to the simple harmonic oscillator example of (1.13), if we fix the correct sparsity structure for both of these methods, we obtain

$$\begin{array}{cc} \text{LSOI + fixed sparsity} & \text{SIDDS + fixed sparsity} \\ \begin{bmatrix} \dot{x}_1 \\ \dot{x}_2 \end{bmatrix} = \begin{bmatrix} 0 & 7.15983089 \\ -5.69559158 & 0 \end{bmatrix} \begin{bmatrix} x_1 \\ x_2 \end{bmatrix} & \begin{bmatrix} \dot{x}_1 \\ \dot{x}_2 \end{bmatrix} = \begin{bmatrix} 0 & 0.99695336 \\ -1.01100718 & 0 \end{bmatrix} \begin{bmatrix} x_1 \\ x_2 \end{bmatrix}. \end{array}$$

Hence fixing the sparsity pattern—equivalent to hard thresholding in STLS—has not improved the parameter estimate using LSOI. Thus sparsity promoting regularization is not sufficient to ensure a method with an LSOI objective term will provide an accurate estimate. Instead, noise must be removed from measurements  $\mathbf{Y}$  so that an accurate estimate of  $\mathbf{C}$  may be obtained.

**1.6. Existing Denoising Work.** There are a wide variety of algorithms for identifying sparse dynamics. We focus our attention on those methods, like ours, that simultaneously estimate the coefficients and true state, or, equivalently, measurement noise. For the most part, these methods do so by adding a penalty based on the dynamical system mismatch rather than adding an equality constraint as with SIDDS. Beyond these methods, there are a variety of techniques that separately denoise measurements and then apply LSOI or a related algorithm; see, e.g., [10]. Although these yield improved performance in the presence of noise, their use requires careful parameter tuning. Hence, we leave a more thorough comparison to future work.

**1.6.1. Sparse Corruption.** A related case to ours where where all measurements have been corrupted by noise, is the case where an unknown (small) fraction of measurements are contaminated by noise. If  $\mathbf{Y} - \mathbf{X}$  has only a few nonzero rows, the dynamical system constraint will similarly be satisfied except for a few nonzero rows; if  $\mathbf{DX} = \Phi(\mathbf{X})\mathbf{C}$ , then the constraint mismatch  $\mathbf{E}$  satisfies

$$(1.16) \quad \mathbf{E} = \Phi(\mathbf{Y})\mathbf{C} - \mathbf{DY} = \Phi(\mathbf{Y} - \mathbf{X})\mathbf{C} - \mathbf{D}(\mathbf{Y} - \mathbf{X}).$$

Tran and Ward propose identifying these corrupted measurements and a sparse dynamical system by solving [30, eq. (9)]

$$(1.17) \quad \begin{array}{l} \min_{\mathbf{C} \in \mathbb{R}^{n \times d}, \mathbf{E} \in \mathbb{R}^{m \times d}} \sum_j \|\mathbf{E}_{j,\cdot}\|_2 \\ \text{s.t. } \mathbf{DY} + \mathbf{E} = \Phi(\mathbf{Y})\mathbf{C} \quad \text{and } \mathbf{C} \text{ sparse} \end{array}$$

where  $\mathbf{E}_{j,\cdot}$  represents the  $j$ th row of  $\mathbf{E}$ . This formulation aims for group-sparsity with respect to the rows of  $\mathbf{E}$  by using a  $\ell_1$  convex relaxation of the  $\ell_0$ -norm in the objective. Although this method does identify the corrupted measurements, it does not identify a corrected state and thus avoids the nonlinearity in  $\Phi$ , working with a fixed  $\Phi(\mathbf{Y})$  rather than our  $\Phi(\mathbf{Z})$ .

**1.6.2. Modified SINDy.** Modified SINDy [20] introduces a variable  $\mathbf{N}$  to estimate the noise and penalizes violation of the dynamical system constraint by the denoised state. Let  $\mathcal{E}^t(\mathbf{x}, \mathbf{C})$  be the evolution operator that advances the differential equation with coefficients  $\mathbf{C}$  from initial condition  $\mathbf{x}$ ,

$$(1.18) \quad \mathcal{E}^t : \mathbb{R}^d \times \mathbb{R}^{n \times d} \rightarrow \mathbb{R}^d, \quad \mathcal{E}^t(\zeta_0, \mathbf{C}) := \zeta(t), \quad \text{where} \quad \begin{cases} \dot{\zeta}(t) = \mathbf{f}(\zeta(t); \mathbf{C}), \\ \zeta(0) = \zeta_0. \end{cases}$$

Modified SINDy then estimates  $\mathbf{C}$  by adding a penalty to LSOI for mismatches in the denoised evolution  $q$  steps forwards and backwards,

(1.19)

$$\min_{\substack{\mathbf{C} \in \mathbb{R}^{n \times d} \\ \mathbf{N} \in \mathbb{R}^{m \times d}}} \|\mathbf{D}(\mathbf{Y} - \mathbf{N}) - \Phi(\mathbf{Y} - \mathbf{N})\mathbf{C}\|_{\text{F}}^2 + \sum_{j=q+1}^{M-q} \sum_{\substack{i=-q \\ i \neq 0}}^q \omega_i \|\mathbf{y}_{j+i} - \mathbf{n}_{j+i} - \mathcal{E}^{\delta i}(\mathbf{y}_j - \mathbf{n}_j, \mathbf{C})\|_2^2$$

where  $\omega_i > 0$  is a weight. Their implementation alternates between minimizing the objective above using stochastic, gradient-based optimization and using STLS to identify a sparsity structure in  $\mathbf{C}$ ; a similar approach is used in [27].

Although more accurate than LSOI, this approach is suboptimal because it imposes the dynamical system constraint through a penalty rather than as an equality constraint. We can observe the loss of accuracy in the simple harmonic oscillator example; using their implementation of Modified SINDy, we recover

Modified SINDy	SIDDS + $\ell_0$
$\begin{bmatrix} \dot{x}_1 \\ \dot{x}_2 \end{bmatrix} = \begin{bmatrix} 0 & 0.91451177 \\ -1.10430015 & 0 \end{bmatrix} \begin{bmatrix} x_1 \\ x_2 \end{bmatrix}$	$\begin{bmatrix} \dot{x}_1 \\ \dot{x}_2 \end{bmatrix} = \begin{bmatrix} 0 & 0.99695336 \\ -1.01100718 & 0 \end{bmatrix} \begin{bmatrix} x_1 \\ x_2 \end{bmatrix}$

Although Modified SINDy vastly outperforms LSOI, the coefficient error is an order of magnitude larger than SIDDS.

**1.6.3. Physics Informed Spline Learning.** Physics Informed Spline Learning (PiSL) [29] uses a similar approach to Modified SINDy, adding a penalty for violating the dynamical system constraint. In PiSL, the estimated state  $\mathbf{z}(t)$  is expressed in a cubic spline basis,  $\mathbf{z}(t) = \mathbf{T}(t)\mathbf{P}$  where  $\mathbf{T}(t)$  is a cubic spline basis and  $\mathbf{P}$  are the control points. To identify the dynamical system, PiSL solves [29, eq. (9)]

$$(1.20) \quad \min_{\mathbf{P}, \mathbf{C}} \frac{1}{m} \sum_{j=1}^m \|\mathbf{y}_j - \mathbf{T}(t_j)\mathbf{P}\|_2^2 + \frac{\alpha}{m} \sum_{j=1}^m \|\dot{\mathbf{T}}(t_j)\mathbf{P} - \sum_{k=1}^n \mathbf{c}_k \phi(\mathbf{T}(t_j)\mathbf{P})\|_2^2 + \beta \|\mathbf{C}\|_0$$

(we omit the stochastic subsampling used in the first two terms in the objective). PiSL's implementation uses a similar approach to Modified SINDy: a minimization alternating between  $\mathbf{P}$  and  $\mathbf{C}$  with a fixed sparsity structure and then applying STLS to identify the sparsity pattern in  $\mathbf{C}$ . Although this method uses a different basis and differs in some details, the overall approach is similar to Modified SINDy.

**1.7. Overview.** The remainder of this manuscript is answers to two questions: what is the statistical performance of SIDDS and how can we efficiently solve the SIDDS optimization problem? First, we convert matrix quantities in (1.10) to vector quantities simplify analysis in section 2. Then in section 3 we obtain a lower bound on the covariance of any dynamical system estimator using the constrained Cramér-Rao Lower Bound (CRLB). We also derive asymptotic estimates of bias and covariance of both SIDDS and LSOI; numerical experiments show SIDDS obtains the CRLB up to discretization error whereas LSOI does not. Next in section 4 we show how to efficiently implement SIDDS using an IRLS approximation to the  $\ell_p$ -norm regularization and a sequential quadratic program (SQP) with a preconditioned MINRES iteration. Finally in section 5, we provide a number of numerical experiments comparing the performance of SIDDS and SIDDS +  $\ell_0$  to LSOI, SINDy with STLS, and Modified SINDy. These experiments show that SIDDS almost exactly obtains the CRLB in a variety of settings whereas existing techniques do not. Moreover, SIDDS +  $\ell_0$  accurately recovers the sparsity structure of  $\mathbf{C}$  at higher levels of noise than other methods. We conclude with a brief discussion of future directions in section 6.

**1.8. Reproducibility.** Following the principles of reproducible research, software implementing our algorithms and the scripts to generate data in the figures are available at <http://github.com/jeffrey-hokanson/sidds>.

**2. Notation and Derivatives.** To follow standard practice in optimization, we reformulate the SIDDS optimization problem with a vector-valued objective and constraint which simplifies the derivations that follow. In this section, we introduce notation for these vectorized quantities, the constraint and its derivative, and generalize the SIDDS optimization problem.

**2.1. Vectorization.** Throughout, we use the row-major vectorization operator

$$(2.1) \quad \text{vec} : \mathbb{R}^{m \times d} \rightarrow \mathbb{R}^{md}, \quad \text{vec}(\mathbf{X}) = \text{vec} \left( \begin{bmatrix} \mathbf{x}_1^\top \\ \vdots \\ \mathbf{x}_m^\top \end{bmatrix} \right) := \begin{bmatrix} \mathbf{x}_1 \\ \vdots \\ \mathbf{x}_m \end{bmatrix}.$$

For brevity, vectorized matrices are denoted by the corresponding lower case letter annotated with a harpoon; e.g.,

$$(2.2) \quad \vec{\mathbf{x}} := \text{vec}(\mathbf{X}), \quad \vec{\mathbf{y}} := \text{vec}(\mathbf{Y}), \quad \vec{\mathbf{z}} := \text{vec}(\mathbf{Z}), \quad \vec{\mathbf{c}} := \text{vec}(\mathbf{C}).$$

Quantities that are still matrices after vectorization are denoted by uppercase letters annotated with a harpoon; e.g.,

$$(2.3) \quad \text{vec}(\Phi(\mathbf{Z})\mathbf{C}) = \vec{\Phi}(\vec{\mathbf{z}})\vec{\mathbf{c}}, \quad \vec{\Phi}(\vec{\mathbf{z}}) := \Phi(\vec{\mathbf{z}}) \otimes \mathbf{I}_d,$$

$$(2.4) \quad \text{vec}(\mathbf{DZ}) = \vec{\mathbf{D}}\vec{\mathbf{z}}, \quad \vec{\mathbf{D}} := \mathbf{D} \otimes \mathbf{I}_d,$$

where  $\otimes$  denotes the Kronecker product and  $\mathbf{I}_d \in \mathbb{R}^{d \times d}$  denotes the identity. The choice of row-major vectorization is important so that  $\vec{\mathbf{D}}$  has low bandwidth. If  $\mathbf{D}$  uses a  $q$ -point stencil, then  $\vec{\mathbf{D}}$  has bandwidth  $d(q-1)$ .

**2.2. Constraint.** The constraint and its derivative are:

$$(2.5) \quad \vec{\mathbf{h}}(\vec{\mathbf{c}}, \vec{\mathbf{z}}) := \text{vec}(\mathbf{DZ} - \Phi(\mathbf{Z})\mathbf{C}) = \vec{\mathbf{D}}\vec{\mathbf{z}} - \vec{\Phi}(\vec{\mathbf{z}})\vec{\mathbf{c}}$$

$$(2.6) \quad \nabla \vec{\mathbf{h}}(\vec{\mathbf{c}}, \vec{\mathbf{z}}) = [\nabla_{\vec{\mathbf{c}}}\vec{\mathbf{h}}(\vec{\mathbf{c}}, \vec{\mathbf{z}}) \quad \nabla_{\vec{\mathbf{z}}}\vec{\mathbf{h}}(\vec{\mathbf{c}}, \vec{\mathbf{z}})] = [-\vec{\Phi}(\vec{\mathbf{z}}) \quad \vec{\mathbf{D}} - \nabla_{\vec{\mathbf{z}}}[\vec{\Phi}(\vec{\mathbf{z}})\vec{\mathbf{c}}]].$$

The last term merits some elaboration. The gradient of  $\vec{\Phi}$  is the 3-tensor  $\nabla \vec{\Phi} : \mathbb{R}^{dm} \rightarrow \mathbb{R}^{(dm) \times (dn) \times (dm)}$ ; thus a Taylor series expansion of  $\vec{\Phi}$  about  $\vec{\mathbf{z}}$  is

$$(2.7) \quad \vec{\Phi}(\vec{\mathbf{z}} + \vec{\delta\mathbf{z}}) = \vec{\Phi}(\vec{\mathbf{z}}) + \nabla \vec{\Phi}(\vec{\mathbf{z}}) \bar{\times}_3 \vec{\delta\mathbf{z}} + \mathcal{O}(\|\vec{\delta\mathbf{z}}\|_2^2),$$

where  $\bar{\times}_3$  denotes tensor multiplication along the third tensor mode [23, subsec. 2.5]. If we take the same Taylor expansion for  $\vec{\Phi}(\vec{\mathbf{z}})\vec{\mathbf{c}}$ ,

$$(2.8) \quad \vec{\Phi}(\vec{\mathbf{z}} + \vec{\delta\mathbf{z}})\vec{\mathbf{c}} = \vec{\Phi}(\vec{\mathbf{z}})\vec{\mathbf{c}} + \left[ \nabla \vec{\Phi}(\vec{\mathbf{z}}) \bar{\times}_3 \vec{\delta\mathbf{z}} \right] \vec{\mathbf{c}} + \mathcal{O}(\|\vec{\delta\mathbf{z}}\|_2^2),$$

we can interchange the order of tensor multiplication yielding

$$(2.9) \quad \vec{\Phi}(\vec{\mathbf{z}} + \vec{\delta\mathbf{z}})\vec{\mathbf{c}} = \vec{\Phi}(\vec{\mathbf{z}})\vec{\mathbf{c}} + \left[ \nabla \vec{\Phi}(\vec{\mathbf{z}}) \bar{\times}_2 \vec{\mathbf{c}} \right] \vec{\delta\mathbf{z}} + \mathcal{O}(\|\vec{\delta\mathbf{z}}\|_2^2).$$

Hence the derivative of  $\vec{\Phi}(\vec{\mathbf{z}})\vec{\mathbf{c}}$  with respect to  $\vec{\mathbf{z}}$  is

$$(2.10) \quad \nabla_{\vec{\mathbf{z}}}[\vec{\Phi}(\vec{\mathbf{z}})\vec{\mathbf{c}}] = \nabla \vec{\Phi}(\vec{\mathbf{z}}) \bar{\times}_2 \vec{\mathbf{c}} \in \mathbb{R}^{(dm) \times (dm)}.$$

This expression allows us to reduce the memory required to compute the constraint derivative; our implementation never explicitly forms the large 3-tensor  $\nabla \vec{\Phi}(\vec{\mathbf{z}})$ , but instead builds  $\nabla \vec{\Phi}(\vec{\mathbf{z}}) \bar{\times}_2 \vec{\mathbf{c}}$  directly.



**2.3. Problem Statement.** Using this vectorized notation, we can restate and generalize the SIDDS+ $\ell_p$  problem (1.15) as

$$(2.11) \quad \begin{aligned} \min_{\vec{\mathbf{c}} \in \mathbb{R}^{dn}, \vec{\mathbf{z}} \in \mathbb{R}^{dm}} & (\vec{\mathbf{y}} - \vec{\mathbf{z}})^\top \vec{\mathbf{M}} (\vec{\mathbf{y}} - \vec{\mathbf{z}}) + \alpha R_p(\vec{\mathbf{c}}) \\ \text{s.t. } & \vec{\mathbf{h}}(\vec{\mathbf{c}}, \vec{\mathbf{z}}) = \vec{\mathbf{D}}\vec{\mathbf{z}} - \vec{\Phi}(\vec{\mathbf{z}})\vec{\mathbf{c}} = \mathbf{0}. \end{aligned}$$

Here the symmetric positive definite matrix  $\vec{\mathbf{M}}$  acts as a weight on the mismatch between the measurements and estimated state. There are two important situations when we might use  $\vec{\mathbf{M}} \neq \mathbf{I}$ . If  $\vec{\mathbf{y}} \sim \mathcal{N}(\vec{\mathbf{x}}, \vec{\Sigma})$ , then taking  $\vec{\mathbf{M}} = \vec{\Sigma}^{-1}$  yields a near optimal estimate for  $\vec{\mathbf{c}}$  and  $\vec{\mathbf{z}}$  as shown in subsection 3.3. The other situation is when we need to decouple the time step used in the ODE constraint from sample rate of measurements in order to improve recovery as illustrated in subsection 5.2.

**3. Statistical Performance.** A key question is: how do methods like SIDDS and LSOI perform when measurements are contaminated by noise? In this section, we analyze these methods when measurements  $\vec{\mathbf{y}}$  have been contaminated with normally distributed additive noise  $\vec{\mathbf{n}}$  with zero mean and full-rank covariance  $\vec{\Sigma}$ ,

$$(3.1) \quad \vec{\mathbf{y}} = \vec{\mathbf{x}} + \vec{\mathbf{n}}, \quad \vec{\mathbf{n}} \sim \mathcal{N}(\vec{\mathbf{0}}, \vec{\Sigma}); \quad \text{equivalently, } \vec{\mathbf{y}} \sim \mathcal{N}(\vec{\mathbf{x}}, \vec{\Sigma}).$$

For these methods, we estimate how  $\vec{\mathbf{c}}$  is perturbed in the limit of small noise and compute the mean and covariance of  $\vec{\mathbf{c}}$  asymptotically. Although only asymptotically valid, numerical experiments show these estimates provide reliable guides to performance. To begin, we compute a lower bound on the covariance of  $\vec{\mathbf{c}}$  based on the solution to the continuous optimization problem. We then compare the asymptotic covariance estimates for LSOI and SIDDS to this lower bound; LSOI is far larger than this lower bound, whereas SIDDS satisfies it almost exactly.

**3.1. Covariance Lower Bound.** Here we use the constrained variant of the Cramér-Rao lower bound to bound the covariance of  $\vec{\mathbf{c}}$ . To begin, let us consider the likelihood function associated with the noise model in (3.1). Suppose our model has estimated the system state sequence  $\vec{\mathbf{z}}$  using coefficients  $\vec{\mathbf{c}}$ ; the corresponding likelihood is

$$(3.2) \quad p(\vec{\mathbf{y}}; \vec{\mathbf{c}}, \vec{\mathbf{z}}) := \det(2\pi\vec{\Sigma})^{-\frac{1}{2}} \exp[-\frac{1}{2}(\vec{\mathbf{y}} - \vec{\mathbf{z}})^\top \vec{\Sigma}^{-1}(\vec{\mathbf{y}} - \vec{\mathbf{z}})];$$

see, e.g., [28, Sec. 2.2]. This likelihood function does not depend on  $\vec{\mathbf{c}}$  explicitly; however  $\vec{\mathbf{z}}$  should satisfy the evolution equations,  $\mathbf{z}_{j+1} = \mathcal{E}^{\delta j}(\mathbf{z}_1, \mathbf{C})$  (recall  $\mathcal{E}$  was defined in (1.18)). We denote this constraint set as

$$(3.3) \quad \Omega := \{\vec{\mathbf{c}}, \vec{\mathbf{z}} : \mathcal{E}^{\delta j}(\mathbf{z}_1, \vec{\mathbf{c}}) = \mathbf{z}_{j+1}, j = 1, \dots, m-1\}.$$

We compute the constrained Cramér-Rao lower bound following [3] using the Fisher information matrix  $\vec{\mathbf{J}}$  and an orthogonal basis for the tangent space of constraints  $\vec{\mathbf{U}}(\vec{\mathbf{c}}, \vec{\mathbf{z}})$ . For this likelihood function (3.2), the Fisher information matrix is constant,

$$(3.4) \quad \vec{\mathbf{J}} := \mathbb{E}_{\vec{\mathbf{y}}} \left[ \nabla_{\vec{\mathbf{c}}, \vec{\mathbf{z}}}^2 \log p(\vec{\mathbf{y}}; \vec{\mathbf{c}}, \vec{\mathbf{z}}) \right] = \begin{bmatrix} \mathbf{0} & \mathbf{0} \\ \mathbf{0} & \vec{\Sigma}^{-1} \end{bmatrix}$$

where  $\mathbb{E}_{\vec{\mathbf{y}}}$  denotes the expectation over  $\vec{\mathbf{y}}$ . Rewriting the constraint set  $\Omega$  in terms of a function  $\vec{\mathbf{h}}_\Omega : \mathbb{R}^{dn} \times \mathbb{R}^{dm} \rightarrow \mathbb{R}^{d(m-1)}$

$$(3.5) \quad \vec{\mathbf{h}}_\Omega(\vec{\mathbf{c}}, \vec{\mathbf{z}}) := \begin{bmatrix} \mathcal{E}^\delta(\mathbf{z}_1, \vec{\mathbf{c}}) - \mathbf{z}_2 \\ \vdots \\ \mathcal{E}^{\delta(m-1)}(\mathbf{z}_1, \vec{\mathbf{c}}) - \mathbf{z}_m \end{bmatrix},$$

the tangent space of the constraint  $\vec{\mathbf{U}}(\vec{\mathbf{c}}, \vec{\mathbf{z}}) \in \mathbb{R}^{(d(m+n)) \times (d(n+1))}$  satisfies

$$(3.6) \quad \mathbf{0} = [\nabla_{\vec{\mathbf{c}}, \vec{\mathbf{z}}} \vec{\mathbf{h}}_{\Omega}(\vec{\mathbf{c}}, \vec{\mathbf{z}})] \vec{\mathbf{U}}(\vec{\mathbf{c}}, \vec{\mathbf{z}}), \quad \text{and} \quad \vec{\mathbf{U}}(\vec{\mathbf{c}}, \vec{\mathbf{z}})^{\top} \vec{\mathbf{U}}(\vec{\mathbf{c}}, \vec{\mathbf{z}}) = \mathbf{I}.$$

Let  $\vec{\mathbf{c}}^*$  and  $\vec{\mathbf{z}}^* = \vec{\mathbf{x}}$  be the true coefficients and states respectively. Then for any estimator that given  $\vec{\mathbf{y}}$  produces unbiased estimates  $\vec{\mathbf{c}}^{\diamond}(\vec{\mathbf{y}})$  and  $\vec{\mathbf{z}}^{\diamond}(\vec{\mathbf{y}})$ , namely,

$$(3.7) \quad \mathbb{E}_{\vec{\mathbf{y}}} \vec{\mathbf{c}}^{\diamond}(\vec{\mathbf{y}}) = \vec{\mathbf{c}}^* \quad \text{and} \quad \mathbb{E}_{\vec{\mathbf{y}}} \vec{\mathbf{z}}^{\diamond}(\vec{\mathbf{y}}) = \vec{\mathbf{z}}^* = \vec{\mathbf{x}},$$

then  $\vec{\mathbf{c}}^{\diamond}$  and  $\vec{\mathbf{z}}^{\diamond}$  satisfy the constrained Cramér-Rao lower bound

$$(3.8) \quad \text{Cov}_{\vec{\mathbf{y}}} \begin{bmatrix} \vec{\mathbf{c}}^{\diamond}(\vec{\mathbf{y}}) \\ \vec{\mathbf{z}}^{\diamond}(\vec{\mathbf{y}}) \end{bmatrix} \succeq \vec{\mathbf{U}}[\vec{\mathbf{U}}^{\top} \vec{\mathbf{J}} \vec{\mathbf{U}}]^+ \vec{\mathbf{U}}^{\top}, \quad \vec{\mathbf{U}} = \vec{\mathbf{U}}(\vec{\mathbf{c}}^*, \vec{\mathbf{z}}^*),$$

where  $\text{Cov}_{\vec{\mathbf{y}}}$  denotes the covariance with respect to  $\vec{\mathbf{y}}$ ,  $^+$  the pseudoinverse [15, Sec. 5.5.2], and  $\succeq$  the ordering of positive semidefinite matrices [19, sec. 7.7].

**3.1.1. Covariance of  $\vec{\mathbf{c}}$ .** As our goal is to estimate the coefficients  $\vec{\mathbf{c}}$ , the estimated state  $\vec{\mathbf{z}}$  is considered a nuisance variable. To compute the covariance of  $\vec{\mathbf{c}}$  alone, we use the selection matrix  $\vec{\mathbf{S}}_{\vec{\mathbf{c}}} \in \mathbb{R}^{(d(m+n)) \times n_c}$  to pick those columns corresponding to  $\vec{\mathbf{c}}$  where  $n_c$  is the number of entries in  $\vec{\mathbf{c}}$  ( $n_c \neq dn$  with a sparsity constraint on  $\vec{\mathbf{c}}$ ). Here,  $\mathbf{S}_{\vec{\mathbf{c}}}$  picks the (1, 1) block of the CRLB:

$$(3.9) \quad \text{Cov } \vec{\mathbf{c}}^{\diamond} \succeq \vec{\mathbf{S}}_{\vec{\mathbf{c}}}^{\top} \vec{\mathbf{U}}[\vec{\mathbf{U}}^{\top} \vec{\mathbf{J}} \vec{\mathbf{U}}]^+ \vec{\mathbf{U}}^{\top} \vec{\mathbf{S}}_{\vec{\mathbf{c}}}.$$

**3.1.2. Sparsity Constraint.** Imposing a sparsity structure on  $\vec{\mathbf{c}}$  changes the Cramér-Rao lower bound as this adds an additional constraint. Suppose  $\mathcal{I}(\vec{\mathbf{c}})$  selects indices of  $\vec{\mathbf{c}}$ ; then setting these entries to zero is equivalent to the constraint set

$$(3.10) \quad \Omega_{\text{sparse}} = \Omega \cap \{\vec{\mathbf{c}}, \vec{\mathbf{z}} : \mathcal{I}(\vec{\mathbf{c}}) = \mathbf{0}\}.$$

As this is a larger set of constraints, this decreases the size of the tangent space. In general, this yields a smaller covariance of the remaining nonzero entries.

**3.1.3. Computing the Tangent Space.** We can compute an orthogonal basis  $\vec{\mathbf{U}}$  for the tangent space of  $\Omega$  by solving the sensitivity equations. Let  $\mathbf{V}$  be the Jacobian with respect to the coefficients  $\vec{\mathbf{c}}$  and  $\mathbf{W}$  be the Jacobian with respect to the initial conditions

$$(3.11) \quad \mathbf{V}(t) = \nabla_{\vec{\mathbf{c}}} \mathcal{E}^t(\mathbf{z}_1, \vec{\mathbf{c}}) \in \mathbb{R}^{d \times n_c}, \quad \mathbf{W}(t) = \nabla_{\mathbf{z}_1} \mathcal{E}^t(\mathbf{z}_1, \vec{\mathbf{c}}) \in \mathbb{R}^{d \times d}.$$

The vectorized versions of these two quantities,  $\vec{\mathbf{v}}(t)$  and  $\vec{\mathbf{w}}(t)$ , evolve according to the coupled differential equations

$$(3.12) \quad \begin{cases} \partial_t \mathbf{z}(t) = \mathbf{f}(\mathbf{z}(t), \vec{\mathbf{c}}) & \mathbf{z}(0) = \mathbf{z}_0 \\ \partial_t \vec{\mathbf{v}}(t) = \mathbf{F}(\mathbf{z}(t), \vec{\mathbf{c}}) \vec{\mathbf{v}}(t) + \nabla_{\vec{\mathbf{c}}} \mathbf{f}(\mathbf{z}(t), \vec{\mathbf{c}}) & \vec{\mathbf{v}}(0) = \mathbf{0} \\ \partial_t \vec{\mathbf{w}}(t) = \mathbf{F}(\mathbf{z}(t), \vec{\mathbf{c}}) \vec{\mathbf{w}}(t) & \vec{\mathbf{w}}(0) = \text{vec}(\mathbf{I}_d) \end{cases}$$

where  $\mathbf{F}(\mathbf{z}, \vec{\mathbf{c}}) = \nabla_{\mathbf{z}} \mathbf{f}(\mathbf{z}, \vec{\mathbf{c}}) = \sum_k \mathbf{c}_k \nabla_{\mathbf{z}} \phi_k(\mathbf{z})$ . Thus the gradient of constraints  $\vec{\mathbf{h}}_{\Omega}$  is

$$(3.13) \quad \nabla_{\vec{\mathbf{c}}, \vec{\mathbf{z}}} \vec{\mathbf{h}}_{\Omega}(\vec{\mathbf{c}}, \vec{\mathbf{z}}) = \nabla_{\vec{\mathbf{c}}, \vec{\mathbf{z}}} \begin{bmatrix} \mathcal{E}^{\delta}(\mathbf{z}_1, \vec{\mathbf{c}}) - \mathbf{z}_2 \\ \mathcal{E}^{2\delta}(\mathbf{z}_1, \vec{\mathbf{c}}) - \mathbf{z}_3 \\ \vdots \\ \mathcal{E}^{m\delta}(\mathbf{z}_1, \vec{\mathbf{c}}) - \mathbf{z}_m \end{bmatrix} = \begin{bmatrix} \mathbf{V}(\delta) & \mathbf{W}(\delta) & -\mathbf{I} & & \\ \mathbf{V}(2\delta) & \mathbf{W}(2\delta) & & -\mathbf{I} & \\ \vdots & \vdots & & & \ddots \\ \mathbf{V}(m\delta) & \mathbf{W}(m\delta) & & & -\mathbf{I} \end{bmatrix}.$$

The structure in this matrix allows us to write down an explicit formula its nullspace,

$$(3.14) \quad \text{Null } \nabla_{\vec{c}, \vec{z}} \vec{h}_\Omega(\vec{c}, \vec{z}) = \text{Range} \left( \begin{bmatrix} \mathbf{I} & \mathbf{0} \\ \mathbf{0} & \mathbf{I} \\ \mathbf{V}(\delta) & \mathbf{W}(\delta) \\ \vdots & \vdots \\ \mathbf{V}(m\delta) & \mathbf{W}(m\delta) \end{bmatrix} \right).$$

Thus we can compute an orthogonal basis for the tangent space of  $\Omega$  at  $\vec{c}, \vec{z}$ , namely,  $\vec{U}(\vec{c}, \vec{z})$ , by performing a reduced QR-factorization of this matrix above.

**3.2. Performance of LSOI.** Let  $\vec{c}^\star$  be the coefficient estimate of LSOI (1.9),

$$(3.15) \quad \vec{c}^\star := \underset{\vec{c}}{\text{argmin}} \|\vec{D}\vec{y} - \vec{\Phi}(\vec{y})\vec{c}\|_2^2.$$

We can alternatively write this solution using the pseudoinverse  $^+$ ,

$$(3.16) \quad \vec{c}^\star = \vec{c}^\star(\vec{y}) = \vec{\Phi}^+(\vec{y})\vec{D}\vec{y}.$$

Assuming  $\vec{y} = \vec{x} + \sigma\vec{n}$  with  $\vec{n} \sim \mathcal{N}(\mathbf{0}, \Sigma)$ , in the limit of small noise ( $\sigma \rightarrow 0$ ),

$$(3.17) \quad \vec{c}^\star = \vec{\Phi}^+(\vec{x} + \sigma\vec{n})\vec{D}(\vec{x} + \sigma\vec{n})$$

$$(3.18) \quad = \vec{\Phi}^+(\vec{x})\vec{D}\vec{x} + \sigma \left( [\nabla\vec{\Phi}^+(\vec{x})]_{\bar{\times}_3} \vec{n} \right) \vec{D}\vec{x} + \sigma\vec{\Phi}^+(\vec{x})\vec{D}\vec{n} + \mathcal{O}(\sigma^2)$$

$$(3.19) \quad = \vec{\Phi}^+(\vec{x})\vec{D}\vec{x} + \sigma \left( [\nabla\vec{\Phi}^+(\vec{x})]_{\bar{\times}_2}(\vec{D}\vec{x}) + \vec{\Phi}^+(\vec{x})\vec{D} \right) \vec{n} + \mathcal{O}(\sigma^2).$$

Let this first order transformation of  $\vec{n}$  be denoted by

$$(3.20) \quad \vec{T}_\star := [\nabla\vec{\Phi}^+(\vec{x})]_{\bar{\times}_2}(\vec{D}\vec{x}) + \vec{\Phi}^+(\vec{x})\vec{D}.$$

To first order,  $\vec{c}^\star$  has a bias proportional to finite difference error in the derivative,

$$(3.21) \quad \mathbb{E}[\vec{c}^\star - \vec{c}^\star] = \vec{\Phi}^+(\vec{x})\vec{D}\vec{x} - \vec{c}^\star + \mathbb{E}_{\vec{n}}[\vec{T}_\star\vec{n}] + \mathcal{O}(\sigma^2)$$

$$(3.22) \quad = \vec{\Phi}^+(\vec{x})(\vec{D}\vec{x} - \dot{\vec{x}}) + \mathcal{O}(\sigma^2),$$

since  $\dot{\vec{x}} = \vec{\Phi}(\vec{x})\vec{c}^\star$  where  $\dot{\vec{x}}$  denotes the state derivative. Similarly, the covariance is

$$(3.23) \quad \text{Cov } \vec{c}^\star = \sigma^2 \vec{T}_\star \vec{\Sigma} \vec{T}_\star^\top + \mathcal{O}(\sigma^3).$$

We can explicitly compute  $\vec{T}_\star$  by using Golub and Pereyra's formula for the derivative of a pseudoinverse [14, eq. (4.12)]; denoting by  $\partial_i$  the derivative of the  $i$ th entry of  $\vec{c}$  and omitting arguments,

$$(3.24) \quad \partial_i \vec{\Phi}^+ = -\vec{\Phi}^+ [\partial_i \vec{\Phi}] \vec{\Phi}^+ + \vec{\Phi}^+ \vec{\Phi}^{+\top} [\partial_i \vec{\Phi}^\top] (\mathbf{I} - \vec{\Phi} \vec{\Phi}^+) + (\mathbf{I} - \vec{\Phi}^+ \vec{\Phi}) [\partial_i \vec{\Phi}^\top] \vec{\Phi}^+ \vec{\Phi}^+.$$

Next, using this asymptotic analysis, we demonstrate LSOI yields suboptimal estimates. In the following examples, we consider the simple harmonic oscillator example from the introduction with a fixed sparsity pattern selecting the true, nonzero values of  $\vec{c}$ . Taking  $\vec{n} \sim \mathcal{N}(\vec{\mathbf{0}}, \sigma^2 \mathbf{I})$  with  $\sigma = 10^{-2}$ , we compute a Monte Carlo estimate of the covariance of  $\vec{c}^\star$ , the asymptotic estimate (3.23), and the Cramér-Rao lower bound (3.9)

Monte Carlo Cov[ $\vec{\mathbf{c}}^\star$ ]	Asymptotic Cov[ $\vec{\mathbf{c}}^\star$ ]	Unbiased CRLB
$\sigma^2 \begin{bmatrix} 0.058709 & 0.001283 \\ 0.001283 & 0.076960 \end{bmatrix}$	$\sigma^2 \begin{bmatrix} 0.057869 & 0.002001 \\ 0.002001 & 0.075413 \end{bmatrix}$	$\sigma^2 \begin{bmatrix} 0.002015 & 0.001990 \\ 0.001990 & 0.002024 \end{bmatrix}$ .

This example shows that the asymptotic estimate provides an accurate covariance and the covariance LSOI is substantially larger than the lower bound. This example used a 3-point finite difference rule; we might expect a higher order finite difference approximation would decrease the covariance. In fact, the opposite happens! Examining the asymptotic covariance for this same problem, we observe

3-point rule Cov[ $\vec{\mathbf{c}}^\star$ ]	5-point rule Cov[ $\vec{\mathbf{c}}^\star$ ]	7-point rule Cov[ $\vec{\mathbf{c}}^\star$ ]
$\sigma^2 \begin{bmatrix} 0.057869 & 0.002001 \\ 0.002001 & 0.075413 \end{bmatrix}$	$\sigma^2 \begin{bmatrix} 0.147962 & 0.002001 \\ 0.002001 & 0.193098 \end{bmatrix}$	$\sigma^2 \begin{bmatrix} 0.943824 & 0.002001 \\ 0.002001 & 1.240532 \end{bmatrix}$ .

The exact origin of this effect is unclear, but it is likely a result of the increased bandwidth of  $\vec{\mathbf{D}}$ . This result provides yet another reason that high order differencing schemes are not frequently seen in other work.

**3.3. Performance of SIDDS.** Here we consider the SIDDS problem with a weighted objective as introduced in (2.11). We will show that by choosing  $\vec{\mathbf{M}} = \vec{\Sigma}^{-1}$ , we obtain estimates that approximately satisfy the CRLB.

As before, we consider the limit of small noise  $\vec{\mathbf{y}} = \vec{\mathbf{x}} + \sigma \vec{\mathbf{n}}$  with  $\sigma \rightarrow 0$  and construct perturbation estimates around the true values

$$(3.25) \quad \vec{\mathbf{c}}^\star = \vec{\mathbf{c}}^\star + \sigma \vec{\mathbf{c}}^{(1)} + \mathcal{O}(\sigma^2) \quad \vec{\mathbf{z}}^\star = \vec{\mathbf{x}} + \sigma \vec{\mathbf{z}}^{(1)} + \mathcal{O}(\sigma^2).$$

Linearizing the constraint of (2.11) around the zeroth order terms yields the quadratic program with Karush-Kuhn-Tucker (KKT) system

$$(3.26) \quad \begin{bmatrix} \mathbf{0} & \vec{\mathbf{K}}^\top & \vec{\mathbf{K}}^\top \\ \sigma^2 \vec{\mathbf{M}} & \vec{\mathbf{L}}^\top & \vec{\mathbf{L}}^\top \\ \vec{\mathbf{K}} & \vec{\mathbf{L}} & \mathbf{0} \end{bmatrix} \begin{bmatrix} \vec{\mathbf{c}}^{(1)} \\ \vec{\mathbf{z}}^{(1)} \\ \vec{\mathbf{w}} \end{bmatrix} = \begin{bmatrix} \vec{\mathbf{0}} \\ \sigma^2 \vec{\mathbf{M}} \vec{\mathbf{n}} \\ -\vec{\mathbf{h}}(\vec{\mathbf{c}}, \vec{\mathbf{x}}) \end{bmatrix}$$

where  $\vec{\mathbf{h}}$  is the constraint defined in (2.5) and  $\vec{\mathbf{K}}$  and  $\vec{\mathbf{L}}$  are the two blocks in the constraint derivative (2.6). To compute  $\vec{\mathbf{c}}^{(1)}$  and  $\vec{\mathbf{z}}^{(1)}$  we use a reduced Hessian approach where  $\vec{\mathbf{U}}_\star$  is an orthogonal basis for the nullspace of  $[\vec{\mathbf{K}} \ \vec{\mathbf{L}}]$ ,

$$(3.27) \quad \begin{bmatrix} \vec{\mathbf{c}}^{(1)} \\ \vec{\mathbf{z}}^{(1)} \end{bmatrix} = -[\vec{\mathbf{K}} \ \vec{\mathbf{L}}]^+ \vec{\mathbf{h}}(\vec{\mathbf{c}}^\star, \vec{\mathbf{x}}) + \vec{\mathbf{U}}_\star \left( \vec{\mathbf{U}}_\star^\top \begin{bmatrix} \mathbf{0} \\ \vec{\mathbf{M}} \end{bmatrix} \vec{\mathbf{U}}_\star \right)^+ \vec{\mathbf{U}}_\star^\top \begin{bmatrix} \vec{\mathbf{0}} \\ \vec{\mathbf{M}} \vec{\mathbf{n}} \end{bmatrix}.$$

As with LSOI, we note that SIDDS has a slight bias since the discretized constraint  $\vec{\mathbf{h}}(\vec{\mathbf{c}}^\star, \vec{\mathbf{x}})$  is not necessarily satisfied exactly

$$(3.28) \quad \mathbb{E} \begin{bmatrix} \vec{\mathbf{c}}^\star - \vec{\mathbf{c}}^\star \\ \vec{\mathbf{z}}^\star - \vec{\mathbf{x}} \end{bmatrix} = -[\vec{\mathbf{K}} \ \vec{\mathbf{L}}]^+ \vec{\mathbf{h}}(\vec{\mathbf{c}}^\star, \vec{\mathbf{x}}) + \mathcal{O}(\sigma^2).$$

Using a higher order finite difference scheme reduces this bias. Returning to the simple harmonic oscillator example with fixed sparsity and  $\vec{\mathbf{n}} \sim \mathcal{N}(\vec{\mathbf{0}}, \vec{\mathbf{I}})$ ,

3-point $\mathbb{E}[\vec{\mathbf{c}}^\star - \vec{\mathbf{c}}^\star]$	5-point $\mathbb{E}[\vec{\mathbf{c}}^\star - \vec{\mathbf{c}}^\star]$	7-point $\mathbb{E}[\vec{\mathbf{c}}^\star - \vec{\mathbf{c}}^\star]$
$\begin{bmatrix} -0.057191 \\ 0.109035 \end{bmatrix}$	$\begin{bmatrix} -1.569746 \cdot 10^{-7} \\ 1.417364 \cdot 10^{-7} \end{bmatrix}$	$\begin{bmatrix} -1.566412 \cdot 10^{-7} \\ 1.414032 \cdot 10^{-7} \end{bmatrix}$ .

Note that this bias almost exactly matches the error in the example in subsection 1.5.

We obtain the asymptotic covariance of the SIDDS estimates by taking the expectation of the outer product of the first order perturbation (3.27),

$$(3.29) \quad \text{Cov} \begin{bmatrix} \vec{\mathbf{c}}^\star \\ \vec{\mathbf{z}}^\star \end{bmatrix} = \vec{\mathbf{U}}_\star \left( \vec{\mathbf{U}}_\star^\top \begin{bmatrix} \mathbf{0} \\ \vec{\mathbf{M}} \end{bmatrix} \vec{\mathbf{U}}_\star \right)^\dagger \vec{\mathbf{U}}_\star^\top \begin{bmatrix} \vec{\mathbf{0}} \\ \sigma^2 \vec{\mathbf{M}} \vec{\Sigma} \vec{\mathbf{M}}^\top \end{bmatrix} \vec{\mathbf{U}}_\star \left( \vec{\mathbf{U}}_\star^\top \begin{bmatrix} \mathbf{0} \\ \vec{\mathbf{M}} \end{bmatrix} \vec{\mathbf{U}}_\star \right)^\dagger \vec{\mathbf{U}}_\star^\top + \mathcal{O}(\sigma^3).$$

If we take  $\vec{\mathbf{M}} = \vec{\Sigma}^{-1}$ , this substantially simplifies:

$$(3.30) \quad \text{Cov} \begin{bmatrix} \vec{\mathbf{c}}^\star \\ \vec{\mathbf{z}}^\star \end{bmatrix} = \vec{\mathbf{U}}_\star \left( \vec{\mathbf{U}}_\star^\top \begin{bmatrix} \mathbf{0} \\ \vec{\Sigma}^{-1} \end{bmatrix} \vec{\mathbf{U}}_\star \right)^\dagger \vec{\mathbf{U}}_\star^\top + \mathcal{O}(\sigma^3), \quad \text{if } \vec{\mathbf{M}} = \vec{\Sigma}^{-1}.$$

This has the same form as (3.8), except the basis for the true tangent space of the ODE constraint  $\vec{\mathbf{U}}$  has been replaced with that of the discretized ODE constraint  $\vec{\mathbf{U}}_\star$ . Typically, the subspace angle between these two spaces is small leading the SIDDS estimate  $\vec{\mathbf{c}}^\star$  to nearly obtain the lower bound. In the simple harmonic oscillator example with fixed sparsity,

3-point Cov $\vec{\mathbf{c}}^\star$	5-point Cov $\vec{\mathbf{c}}^\star$	Unbiased CRLB
$\begin{bmatrix} 0.002007 & 0.001995 \\ 0.001995 & 0.002004 \end{bmatrix}$	$\begin{bmatrix} 0.002015 & 0.001990 \\ 0.001990 & 0.002024 \end{bmatrix}$	$\begin{bmatrix} 0.002015 & 0.001990 \\ 0.001990 & 0.002024 \end{bmatrix}$

Unlike LSOI, higher order difference schemes for SIDDS yield better estimates. Note that the 3-point covariance is slightly smaller than the unbiased Cramér-Rao lower bound which is possible due to its bias; the 5-point covariance matches the lower bound with an error around  $10^{-7}$ .

**4. Solving SIDDS.** We now turn our attention to devising an efficient numerical algorithm to solve the SIDDS optimization problem:

$$(4.1) \quad \begin{aligned} \min_{\vec{\mathbf{c}}, \vec{\mathbf{z}}} & (\vec{\mathbf{y}} - \vec{\mathbf{z}})^\top \vec{\mathbf{M}} (\vec{\mathbf{y}} - \vec{\mathbf{z}}) + \alpha R_p(\vec{\mathbf{c}}) & \text{recall } R_p(\vec{\mathbf{c}}) := \begin{cases} \|\vec{\mathbf{c}}\|_p^p, & p > 0; \\ \|\vec{\mathbf{c}}\|_0, & p = 0; \end{cases} \\ \text{s.t. } & \vec{\mathbf{D}} \vec{\mathbf{z}} = \vec{\Phi}(\vec{\mathbf{z}}) \vec{\mathbf{c}}; \end{aligned}$$

and  $\vec{\mathbf{M}} \in \mathbb{R}^{(dm) \times (dm)}$  is positive semidefinite. Structurally, this problem is close to a quadratic program, and would be if  $\vec{\Phi}(\vec{\mathbf{z}})$  was held constant and regularization removed ( $\alpha = 0$ ). Hence, we will use a SQP approach to solve SIDDS. However, rather than optimizing (4.1) directly, we will use IRLS to provide a convex approximation of  $R_p$  as described in subsection 4.2. We then use the SQP approach of Lin and Yuan [25] to optimize the IRLS approximated problem, taking special care to exploit structure; we discuss this in subsection 4.3. We then show how this approach can be extended to problems where multiple trajectories in subsection 4.4. We begin by discussing how initialize this nonconvex optimization problem.

**4.1. Initialization.** Since (4.1) is a nonconvex optimization problem, convergence to a global optimum from arbitrary initial estimates is not guaranteed. With small noise, simply taking  $\vec{\mathbf{z}}^{(0)} = \vec{\mathbf{y}}$  and  $\vec{\mathbf{c}}^{(0)} = \mathbf{0}$  (superscripts denoting iteration number) yields good local minimizers. With large noise, we find better solutions by applying modest amount of smoothing. In particular, we use Tikhonov smoothing,

$$(4.2) \quad \vec{\mathbf{z}}^{(0)} = \underset{\vec{\mathbf{z}}}{\text{argmin}} \left\| \begin{bmatrix} \vec{\mathbf{y}} \\ \mathbf{0} \end{bmatrix} - \begin{bmatrix} \mathbf{I} \\ \lambda \vec{\mathbf{D}}^2 \end{bmatrix} \vec{\mathbf{z}} \right\|_2^2$$

**Algorithm 4.1** SIDDS with IRLS Regularization Approximation

---

**Input** : measurements  $\vec{\mathbf{y}}$ , regularization order  $p \geq 0$ , basis functions  $\{\phi_k\}_{k=1}^n$ , regularization weight  $\alpha \geq 0$ , truncation parameter  $\tau \geq 0$

**Output** : parameter estimates  $\vec{\mathbf{c}}$ , denoised state  $\vec{\mathbf{z}}$

- 1 Initialize  $\epsilon^{(0)} \leftarrow 1$ ,  $\vec{\mathbf{z}}^{(0)}$  by smoothing (4.2),  $\vec{\mathbf{c}}^{(0)}$  by LSOI (1.9) applied to  $\vec{\mathbf{z}}^{(0)}$ ;
- 2 **for**  $\ell = 1, 2, 3, \dots$  **do**
- 3      $\vec{\mathbf{W}}^{(\ell-1)} \leftarrow \text{diag}(|\vec{\mathbf{c}}^{(\ell-1)}|^2 + \epsilon^{(\ell-1)})^{\frac{p}{2}-1}$ ;
- 4     Obtain  $\vec{\mathbf{c}}^{(\ell)}$  and  $\vec{\mathbf{z}}^{(\ell)}$  by one step of SQP applied to  

$$\min_{\vec{\mathbf{c}}, \vec{\mathbf{z}}} (\vec{\mathbf{y}} - \vec{\mathbf{z}})^\top \vec{\mathbf{M}}(\vec{\mathbf{y}} - \vec{\mathbf{z}}) + \alpha \vec{\mathbf{c}}^\top \vec{\mathbf{W}}^{(\ell-1)} \vec{\mathbf{c}} \quad \text{s.t.} \quad \vec{\mathbf{D}} \vec{\mathbf{z}} = \vec{\Phi}(\vec{\mathbf{z}}) \vec{\mathbf{c}};$$
- 5     **if** *optimization converged* **then**  $\epsilon^{(\ell)} \leftarrow \epsilon^{(\ell-1)}/10$ ;
- 6     **else**  $\epsilon^{(\ell)} \leftarrow \epsilon^{(\ell-1)}$ ;
- 7     **if** *optimization converged and*  $\epsilon^{(\ell)} < 10^{-8}$  **then break**;
- 8 Fix sparsity structure in  $\vec{\mathbf{c}}$  setting  $c_i = 0$  if  $|c_i| \leq \tau$  and solve  

$$\min_{\vec{\mathbf{c}}, \vec{\mathbf{z}}} (\vec{\mathbf{y}} - \vec{\mathbf{z}})^\top \vec{\mathbf{M}}(\vec{\mathbf{y}} - \vec{\mathbf{z}}) \quad \text{s.t.} \quad \vec{\mathbf{D}} \vec{\mathbf{z}} = \vec{\Phi}(\vec{\mathbf{z}}) \vec{\mathbf{c}};$$

---

where  $\lambda > 0$  is a smoothing parameter (in our experiments  $\lambda = 10^{-2}$ ) and  $\vec{\mathbf{D}}^2$  is a 3-point finite-difference approximation of the second derivative. Then we apply LSOI to estimate  $\vec{\mathbf{c}}^{(0)}$  based on  $\vec{\mathbf{z}}^{(0)}$ .

**4.2. Approximating Regularization via IRLS.** The regularization  $R_p$  in the objective (4.1) presents a challenge: for  $p < 1$ ,  $R_p$  is concave introducing negative curvature into the Hessian of the objective. To avoid this difficulty, we replace  $R_p$  with an IRLS approximation [4, subsec. 4.5.2] yielding a positive semidefinite Hessian. At the  $\ell$ th iterate, the IRLS approximation of  $R_p$  is

$$(4.3) \quad R_p(\vec{\mathbf{c}}^{(\ell)}) := \sum_i |c_i^{(\ell)}|^p = \sum_i |c_i^{(\ell)}|^{p-2} |c_i^{(\ell)}|^2 \approx \sum_i |c_i^{(\ell-1)}|^{p-2} |c_i^{(\ell)}|^2.$$

If  $\vec{\mathbf{c}}^{(\ell-1)} \rightarrow \vec{\mathbf{c}}^{(\ell)}$  as  $\ell \rightarrow \infty$ , this IRLS approximation approaches  $R_p$ . Numerically, when  $c_i^{(\ell-1)}$  is small and  $p < 2$ , we can encounter a divide by zero error. Following Chartrand and Yin [8], we avoid this by introducing an iteration dependent regularization  $\epsilon^{(\ell)} > 0$ ; this yields the quadratic approximation:

$$(4.4) \quad R_p(\vec{\mathbf{c}}) \approx R_p^{(\ell)}(\vec{\mathbf{c}}) := \vec{\mathbf{c}}^\top \vec{\mathbf{W}}^{(\ell-1)} \vec{\mathbf{c}}, \quad \vec{\mathbf{W}}^{(\ell)} := \text{diag} \left( \left\{ [ |c_i^{(\ell)}|^2 + \epsilon^{(\ell)} ]^{\frac{p}{2}-1} \right\}_i \right).$$

As the optimization proceeds, we let  $\epsilon^{(\ell)} \rightarrow 0$ . We opt for the simple heuristic of decreasing  $\epsilon$  by a factor of ten when optimization terminates successfully following [8], although more sophisticated heuristics exist [11, 24]. Then once  $\epsilon$  is sufficiently small, we fix the sparsity structure by setting small entries in  $\vec{\mathbf{c}}$  to zero and continue optimization until the termination conditions are met. This final polishing step removes the bias introduced by the regularization. This process is summarized in Algorithm 4.1.

Figure 4.1 shows how SIDDS proceeds using this IRLS approximation approach. Starting with large regularization  $\epsilon = 1$ , the optimizer rapidly identifies a good approximation of the true state, which then slowly improves over the course of optimization. Then, as the IRLS regularization term decreases we slowly obtain better coefficient estimates. After each decrease of regularization, we first see an increase in

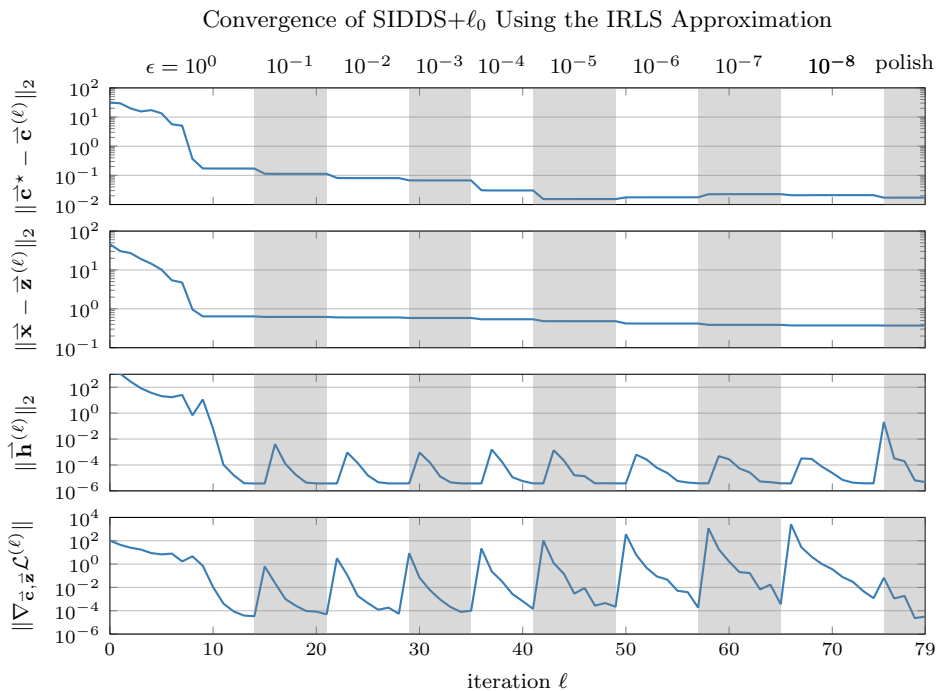


FIG. 4.1. Using the IRLS approximation of  $R_0$  regularization, we rapidly identify the dynamical system to high accuracy. Stripes denote the different values of  $\epsilon$  used as regularization of the IRLS approximation of the  $\ell_0$ -norm. The bottom plot measures the first order optimality of the solution, where  $\mathcal{L}^{(\ell)}$  is the Lagrangian (4.20) at the  $\ell$ -th iterate. The data for this problem corresponds to the Lorenz 63 attractor example introduced in subsection 5.1.2 with additive i.i.d. normally distributed noise with standard deviation  $\sigma = 0.1$  and  $m = 2000$  measurements.

the Lagrangian gradient norm, followed by an increase in the constraint mismatch at the subsequent iteration. However, after only a few more iterations, the optimization converges for this particular  $\epsilon$  and the value of  $\epsilon$  is decreased.

**4.3. Performing SQP Steps.** Using the IRLS convex approximation of the  $\ell_p$ -norm constraint, we now seek to solve the corresponding optimization problem,

$$(4.5) \quad \begin{aligned} \min_{\vec{c}, \vec{z}} f(\vec{c}, \vec{z}) &:= \frac{1}{2}(\vec{y} - \vec{z})^\top \vec{M}(\vec{y} - \vec{z}) + \frac{\alpha}{2} \vec{c}^\top \vec{W}^{(\ell)} \vec{c}, \\ \text{s.t. } \vec{h}(\vec{c}, \vec{z}) &:= \vec{D} \vec{z} - \vec{\Phi}(\vec{z}) \vec{c} = \mathbf{0}. \end{aligned}$$

Here we use the SQP approach of Liu and Yuan [25] to ensure convergence without the use of a merit function or filter. Each step of their algorithm requires the solution of two large-scale subproblems: a relaxation step and quadratic subproblem. We show how both can be efficiently solved by exploiting the structure of the SIDDS optimization problem.

**4.3.1. Relaxation Step.** The relaxation step seeks to find a direction  $\vec{p}^{(\ell)}$  that approximately minimizes the error in the linearization of the constraints:

$$(4.6) \quad \vec{p}^{(\ell)} \approx \underset{\vec{p}}{\operatorname{argmin}} \|\vec{h}^{(\ell)} + \vec{A}^{(\ell)} \vec{p}\|_2^2,$$

$$(4.7) \quad \text{where } \vec{A}^{(\ell)} := \vec{A}(\vec{c}^{(\ell)}, \vec{z}^{(\ell)}), \quad \vec{A}(\vec{c}, \vec{z}) := [\nabla_{\vec{c}} \vec{h}(\vec{c}, \vec{z}) \quad \nabla_{\vec{z}} \vec{h}(\vec{c}, \vec{z})],$$

and  $\vec{\mathbf{h}}^{(\ell)} := \vec{\mathbf{h}}(\vec{\mathbf{c}}^{(\ell)}, \vec{\mathbf{z}}^{(\ell)})$ . For the convergence analysis of [25] to hold, this direction  $\vec{\mathbf{p}}^{(\ell)}$  must satisfy two constraints for small constants  $\kappa_1$  and  $\kappa_2$

$$(4.8) \quad \|\vec{\mathbf{p}}^{(\ell)}\| \leq \kappa_1 \|\vec{\mathbf{A}}^{(\ell)\top} \vec{\mathbf{h}}^{(\ell)}\|, \quad \kappa_1 \geq 0;$$

$$(4.9) \quad \|\vec{\mathbf{h}}^{(\ell)}\|^2 - \|\vec{\mathbf{h}}^{(\ell)}\| \|\vec{\mathbf{h}}^{(\ell)} + \vec{\mathbf{A}}^{(\ell)} \vec{\mathbf{p}}^{(\ell)}\| \geq \kappa_2 \|\vec{\mathbf{A}}^{(\ell)\top} \vec{\mathbf{h}}^{(\ell)}\|^2, \quad \kappa_2 \in (0, 1).$$

Due to the scale of  $\vec{\mathbf{A}} \in \mathbb{R}^{(dn) \times (dm+dn)}$ , direct solution methods for (4.6) are impractical. Instead, we compute the relaxation step by exploiting the structure of  $\vec{\mathbf{A}}^{(\ell)}$ . The matrix  $\vec{\mathbf{A}}^{(\ell)}$  contains two blocks,  $\vec{\mathbf{A}}^{(\ell)} = [\vec{\mathbf{K}}^{(\ell)} \quad \vec{\mathbf{L}}^{(\ell)}]$ , where

$$(4.10) \quad \vec{\mathbf{K}}^{(\ell)} := \vec{\mathbf{K}}(\vec{\mathbf{c}}^{(\ell)}, \vec{\mathbf{z}}^{(\ell)}), \quad \vec{\mathbf{K}}(\vec{\mathbf{c}}, \vec{\mathbf{z}}) := \nabla_{\vec{\mathbf{c}}} \vec{\mathbf{h}}(\vec{\mathbf{c}}, \vec{\mathbf{z}}) = -\vec{\Phi}(\vec{\mathbf{z}});$$

$$(4.11) \quad \vec{\mathbf{L}}^{(\ell)} := \vec{\mathbf{L}}(\vec{\mathbf{c}}^{(\ell)}, \vec{\mathbf{z}}^{(\ell)}), \quad \vec{\mathbf{L}}(\vec{\mathbf{c}}, \vec{\mathbf{z}}) := \nabla_{\vec{\mathbf{z}}} \vec{\mathbf{h}}(\vec{\mathbf{c}}, \vec{\mathbf{z}}) = \vec{\mathbf{D}} - \nabla \Phi(\vec{\mathbf{z}}) \times_2 \vec{\mathbf{c}}.$$

Our approach is to split  $\vec{\mathbf{p}}$  into components corresponding to  $\vec{\mathbf{c}}$  and  $\vec{\mathbf{z}}$ :

$$(4.12) \quad \|\vec{\mathbf{h}}^{(\ell)} + \vec{\mathbf{A}}^{(\ell)} \vec{\mathbf{p}}\|_2^2 = \|\vec{\mathbf{h}}^{(\ell)} + \vec{\mathbf{K}}^{(\ell)} \vec{\mathbf{p}}_{\vec{\mathbf{c}}} + \vec{\mathbf{L}}^{(\ell)} \vec{\mathbf{p}}_{\vec{\mathbf{z}}}\|_2^2 \quad \text{where} \quad \vec{\mathbf{p}} = \begin{bmatrix} \vec{\mathbf{p}}_{\vec{\mathbf{c}}} \\ \vec{\mathbf{p}}_{\vec{\mathbf{z}}} \end{bmatrix}$$

and then solve for  $\vec{\mathbf{p}}_{\vec{\mathbf{c}}}$  and  $\vec{\mathbf{p}}_{\vec{\mathbf{z}}}$  separately.

We compute  $\vec{\mathbf{p}}_{\vec{\mathbf{c}}}^{(\ell)}$  by setting  $\vec{\mathbf{p}}_{\vec{\mathbf{z}}} = \mathbf{0}$  and solving the overdetermined least squares problem

$$(4.13) \quad \vec{\mathbf{p}}_{\vec{\mathbf{c}}}^{(\ell)} := \operatorname{argmin}_{\vec{\mathbf{p}}_{\vec{\mathbf{c}}}} \|\vec{\mathbf{h}}^{(\ell)} + \vec{\mathbf{K}}^{(\ell)} \vec{\mathbf{p}}_{\vec{\mathbf{c}}}\|_2^2$$

$$(4.14) \quad = \operatorname{argmin}_{\vec{\mathbf{p}}_{\vec{\mathbf{c}}}} \|\vec{\Phi}(\vec{\mathbf{z}}^{(\ell)}) \vec{\mathbf{p}}_{\vec{\mathbf{c}}} - [\vec{\mathbf{D}} \vec{\mathbf{z}}^{(\ell)} - \vec{\Phi}(\vec{\mathbf{z}}^{(\ell)}) \vec{\mathbf{c}}^{(\ell)}]\|_2^2.$$

This second statement has the same structure as LSOI (1.9) allowing us to restate this in a dense matrix format, removing the Kronecker products:

$$(4.15) \quad \mathbf{P}_{\vec{\mathbf{c}}}^{(\ell)} := \operatorname{argmin}_{\mathbf{P}_{\vec{\mathbf{c}}}} \|\Phi(\mathbf{Z}^{(\ell)}) \mathbf{P}_{\vec{\mathbf{c}}} - [\mathbf{DZ}^{(\ell)} - \Phi(\mathbf{Z}^{(\ell)}) \mathbf{C}^{(\ell)}]\|_{\mathbf{F}}^2.$$

This allows more efficient solution via a QR factorization and we set  $\vec{\mathbf{p}}_{\vec{\mathbf{c}}}^{(\ell)} = \operatorname{vec}(\mathbf{P}_{\vec{\mathbf{c}}}^{(\ell)})$ .

Next, we solve for  $\vec{\mathbf{p}}_{\vec{\mathbf{z}}}$  holding  $\vec{\mathbf{p}}_{\vec{\mathbf{c}}}$  constant:

$$(4.16) \quad \vec{\mathbf{p}}_{\vec{\mathbf{z}}}^{(\ell)} \approx \operatorname{argmin}_{\vec{\mathbf{p}}_{\vec{\mathbf{z}}}} \|\vec{\mathbf{h}}^{(\ell)} + \vec{\mathbf{K}}^{(\ell)} \vec{\mathbf{p}}_{\vec{\mathbf{c}}}^{(\ell)} + \vec{\mathbf{L}}^{(\ell)} \vec{\mathbf{p}}_{\vec{\mathbf{z}}}\|_2^2.$$

Although  $\vec{\mathbf{L}}^{(\ell)}$  is square, it is structurally rank deficient. The matrix  $\vec{\mathbf{L}}^{(\ell)}$  encodes the discretized constraint for  $\mathcal{E}^{\delta(j-1)}(\mathbf{z}_1, \vec{\mathbf{c}}) = \mathbf{z}_j$  for  $j = 2, \dots, m$ ; this continuous constraint only provides  $d(m-1)$  constraints whereas  $\vec{\mathbf{L}}^{(\ell)}$  encodes  $dm$  constraints. Thus when approximating  $\vec{\mathbf{p}}_{\vec{\mathbf{z}}}$  we include a small amount of Tikhonov regularization and solve via the normal equations:

$$(4.17) \quad \vec{\mathbf{p}}_{\vec{\mathbf{z}}}^{(\ell)} := -[\vec{\mathbf{L}}^{(\ell)\top} \vec{\mathbf{L}}^{(\ell)} + \beta \mathbf{I}]^{-1} \vec{\mathbf{L}}^{(\ell)\top} [\vec{\mathbf{h}}^{(\ell)} + \vec{\mathbf{K}}^{(\ell)} \vec{\mathbf{p}}_{\vec{\mathbf{c}}}^{(\ell)}];$$

in our numerical experiments we take  $\beta = 10^{-6}$ . Since  $\vec{\mathbf{L}}^{(\ell)} \in \mathbb{R}^{(dm) \times (dm)}$  has small bandwidth  $dq \ll dm$ , we efficiently apply its inverse using a sparse LU factorization.



**4.3.2. Solution of Quadratic Subproblem.** The other expensive component of the Liu and Yuan SQP algorithm is solving the relaxed quadratic program

$$(4.18) \quad \begin{aligned} \vec{\mathbf{d}}^{(\ell)} &= \underset{\vec{\mathbf{d}}}{\operatorname{argmin}} \vec{\mathbf{g}}^{(\ell)\top} \vec{\mathbf{d}} + \frac{1}{2} \vec{\mathbf{d}}^\top \vec{\mathbf{B}}^{(\ell)} \vec{\mathbf{d}} \\ \text{s.t. } \vec{\mathbf{A}}^{(\ell)} \vec{\mathbf{d}} &= \vec{\mathbf{A}}^{(\ell)} \vec{\mathbf{p}}^{(\ell)} \end{aligned}$$

where  $\vec{\mathbf{B}}^{(\ell)}$  is an approximation of the Lagrangian Hessian and  $\vec{\mathbf{g}}^{(\ell)}$  is the gradient

$$(4.19) \quad \vec{\mathbf{g}}^{(\ell)} := \vec{\mathbf{g}}(\vec{\mathbf{c}}^{(\ell)}, \vec{\mathbf{z}}^{(\ell)}) \quad \vec{\mathbf{g}}(\vec{\mathbf{c}}, \vec{\mathbf{z}}) := [\nabla_{\vec{\mathbf{c}}} f(\vec{\mathbf{c}}, \vec{\mathbf{z}}) \quad \nabla_{\vec{\mathbf{z}}} f(\vec{\mathbf{c}}, \vec{\mathbf{z}})].$$

Here we introduce a sparse approximation of the  $\vec{\mathbf{B}}^{(\ell)}$  and show how to efficiently solve (4.18) by direct solution of the stabilized KKT system with a preconditioned MINRES iteration.

Ideally we would use the exact Hessian of the Lagrangian for  $\vec{\mathbf{B}}^{(\ell)}$

$$(4.20) \quad \mathcal{L}(\vec{\mathbf{c}}, \vec{\mathbf{z}}, \vec{\mathbf{w}}) := f(\vec{\mathbf{c}}, \vec{\mathbf{z}}) + \vec{\mathbf{w}}^\top \vec{\mathbf{h}}(\vec{\mathbf{c}}, \vec{\mathbf{z}}),$$

where  $\vec{\mathbf{w}}$  are the Lagrange multipliers. However, this choice is impractical as  $\nabla_{\vec{\mathbf{c}}, \vec{\mathbf{z}}}^2 \mathcal{L}$  will generally be dense. Note the contribution from the Lagrange multiplier term is

$$(4.21) \quad \vec{\mathbf{w}}^\top \vec{\mathbf{h}}(\vec{\mathbf{c}}, \vec{\mathbf{z}}) = \vec{\mathbf{w}}^\top \vec{\mathbf{D}}_p \vec{\mathbf{z}} - \vec{\mathbf{w}}^\top \vec{\Phi}(\vec{\mathbf{z}}) \vec{\mathbf{c}};$$

the Hessian of this second term  $\vec{\mathbf{w}}^\top \vec{\Phi}(\vec{\mathbf{z}}) \vec{\mathbf{c}}$  will be dense except for special combinations of  $\vec{\mathbf{c}}$  and basis vectors  $\phi_k$ . Instead we neglect this term entirely and approximate the Hessian of the Lagrangian by the Hessian of the objective:

$$(4.22) \quad \vec{\mathbf{B}}^{(\ell)} := \nabla_{\vec{\mathbf{c}}, \vec{\mathbf{z}}}^2 f(\vec{\mathbf{c}}^{(\ell)}, \vec{\mathbf{z}}^{(\ell)}) = \begin{bmatrix} \alpha \vec{\mathbf{W}}^{(\ell)} & \mathbf{0} \\ \mathbf{0} & \vec{\mathbf{M}} \end{bmatrix}.$$

By construction, this is a positive semidefinite matrix.

Next, we seek to solve the KKT system

$$(4.23) \quad \begin{bmatrix} \vec{\mathbf{B}}^{(\ell)} & \vec{\mathbf{A}}^{(\ell)\top} \\ \vec{\mathbf{A}}^{(\ell)} & \mathbf{0} \end{bmatrix} \begin{bmatrix} \vec{\mathbf{d}} \\ \vec{\mathbf{w}} \end{bmatrix} = \begin{bmatrix} -\vec{\mathbf{g}}^{(\ell)} \\ \vec{\mathbf{A}}^{(\ell)} \vec{\mathbf{p}}^{(\ell)} \end{bmatrix}.$$

Since  $\vec{\mathbf{L}}^{(\ell)}$  is rank deficient,  $\vec{\mathbf{A}}^{(\ell)}$  does not have full row rank causing the KKT system to be singular. To correct this, we use a stabilization procedure following Wright [31, eq. (4.2)] where we add multiple of the identity to the (1, 1) and (2, 2) blocks,

$$(4.24) \quad \begin{bmatrix} \vec{\mathbf{B}}^{(\ell)} + \zeta \mathbf{I} & \vec{\mathbf{A}}^{(\ell)\top} \\ \vec{\mathbf{A}}^{(\ell)} & -\gamma^{(\ell)} \mathbf{I} \end{bmatrix} \begin{bmatrix} \vec{\mathbf{d}}^{(\ell)} \\ \vec{\mathbf{w}}^{(\ell)} \end{bmatrix} = \begin{bmatrix} -\vec{\mathbf{g}}^{(\ell)} \\ \vec{\mathbf{A}}^{(\ell)} \vec{\mathbf{p}}^{(\ell)} \end{bmatrix}.$$

In our implementation we fix  $\zeta = 10^{-4}$  and scale  $\gamma$  based on the previous iteration

$$(4.25) \quad \gamma^{(\ell)} = 10^{-4} \left( \|\vec{\mathbf{g}}^{(\ell-1)} + \vec{\mathbf{w}}^{(\ell-1)} \vec{\mathbf{A}}^{(\ell-1)}\|_1 + \|\vec{\mathbf{h}}^{(\ell-1)}\|_1 \right).$$

To solve (4.24), we use a preconditioned MINRES iteration following Alger, et al. [1]. This preconditioner is derived from a block-diagonal approximation of the KKT system corresponding the augmented objective,

$$(4.26) \quad f_\mu(\vec{\mathbf{c}}, \vec{\mathbf{z}}) := f(\vec{\mathbf{c}}, \vec{\mathbf{z}}) + \mu \|\vec{\mathbf{h}}(\vec{\mathbf{c}}, \vec{\mathbf{z}})\|_2^2$$

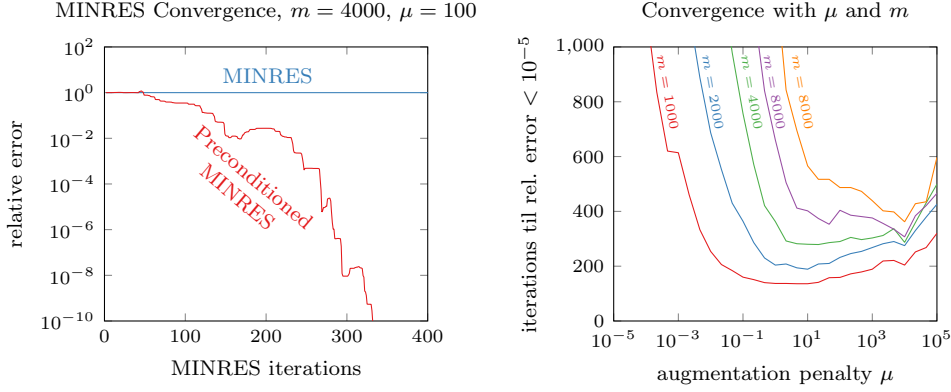


FIG. 4.2. The preconditioner  $\mathcal{M}$  accelerates the convergence of MINRES on the KKT system (4.24). On the left we show the convergence the MINRES iteration by showing the 2-norm difference between each iterate’s estimate of the solution and the converged value. On the right, we see the number of MINRES iterations required varies as a function of augmentation penalty  $\mu$  and problem dimension  $m$ . Test data comes from the Van der Pol oscillator described in subsection 5.1.3.

for some penalty  $\mu > 0$ . In our setting, this preconditioner is

$$(4.27) \quad \mathcal{M}^{(\ell)} = \begin{bmatrix} \alpha \vec{\mathbf{W}} + \zeta \mathbf{I} + \mu \vec{\mathbf{K}}^{(\ell)\top} \vec{\mathbf{K}}^{(\ell)} & \\ & \vec{\mathbf{M}} + \zeta \mathbf{I} + \mu \vec{\mathbf{L}}^{(\ell)\top} \vec{\mathbf{L}}^{(\ell)} \\ & & \frac{1}{\mu} \mathbf{I} \end{bmatrix}.$$

We can efficiently apply  $\mathcal{M}^{(\ell)-1}$  blockwise. The first block is small,  $dn$ , so we explicitly compute its inverse. The second block is large,  $dm$ , but low bandwidth  $dq \ll dm$ , so we apply its inverse by precomputing a sparse factorization; in our experiments an LU factorization computed using SuperLU [13]. As illustrated in Figure 4.2, this preconditioner enables rapid solution of the KKT system. In our setting, the performance of this preconditioner depends on the augmentation penalty  $\mu$ . These experiments show that a value  $\mu \in [10, 1000]$  enables fast convergence for a variety of problem dimensions; our experiments take  $\mu = 100$ .

**4.4. Multiple Trajectories.** In some situations it is necessary incorporate data from multiple trajectories to ensure the operator inference problem is well posed [32]. For example, a single trajectory might not sufficiently explore the state-space to enable an accurate estimate of the parameters  $\vec{\mathbf{c}}$ . Fortunately, SIDDS can be easily modified to accommodate this situation. Suppose we have trajectories  $\{\vec{\mathbf{y}}_{(i)}\}_{i=1}^N$ , we then seek to solve an extension of (4.5)

$$(4.28) \quad \begin{aligned} \vec{\mathbf{c}}, \vec{\mathbf{z}}_{(1)}, \dots, \vec{\mathbf{z}}_{(N)} \quad & \sum_{i=1}^N \frac{1}{2} [\vec{\mathbf{y}}_{(i)} - \vec{\mathbf{z}}_{(i)}]^\top \vec{\mathbf{M}}_{(i)} [\vec{\mathbf{y}}_{(i)} - \vec{\mathbf{z}}_{(i)}] + \frac{\alpha}{2} \vec{\mathbf{c}}^\top \vec{\mathbf{W}} \vec{\mathbf{c}}, \\ \text{s.t. } \vec{\mathbf{D}}_p \vec{\mathbf{z}}_{(i)} - \vec{\Phi}(\vec{\mathbf{z}}_{(i)}) \vec{\mathbf{c}} &= \mathbf{0}, \quad i = 1, \dots, N. \end{aligned}$$

Structurally, this optimization problem is similar to (4.5) enabling us to use the same techniques to efficiently solve this problem. We build the constraint derivative using components defined analogously to (4.10) and (4.11),

$$(4.29) \quad \vec{\mathbf{K}}_{(i)}^{(\ell)} := -\vec{\Phi}(\vec{\mathbf{z}}_{(i)}^{(\ell)}), \quad \vec{\mathbf{L}}_{(i)}^{(\ell)} := \vec{\mathbf{D}}_p - [\nabla \vec{\Phi}(\vec{\mathbf{z}}_{(i)}^{(\ell)}) \bar{\times}_2 \vec{\mathbf{c}}^{(\ell)}],$$

forming the full constraint derivative,

$$(4.30) \quad \vec{\mathbf{A}}^{(\ell)} := \begin{bmatrix} \vec{\mathbf{K}}_{(1)}^{(\ell)} & \vec{\mathbf{L}}_{(1)}^{(\ell)} & & \\ \vdots & & \ddots & \\ \vec{\mathbf{K}}_{(N)}^{(\ell)} & & & \vec{\mathbf{L}}_{(N)}^{(\ell)} \end{bmatrix}.$$

$\underbrace{\hspace{10em}}_{\vec{\mathbf{K}}_{\square}^{(\ell)}} \quad \underbrace{\hspace{10em}}_{\vec{\mathbf{L}}_{\square}^{(\ell)}}$

These two matrices  $\vec{\mathbf{K}}_{\square}^{(\ell)}$  and  $\vec{\mathbf{L}}_{\square}^{(\ell)}$  with a dense rectangular block and a sparse, low-bandwidth square matrix can be used analogously in place of  $\vec{\mathbf{K}}^{(\ell)}$  and  $\vec{\mathbf{L}}^{(\ell)}$  in the preceding analysis for the relaxation step and the quadratic subproblem. This enables an efficient solution to SIDDS with multiple trajectory data.

**5. Numerical Experiments.** In this section we provide a few numerical experiments illustrating the performance of SIDDS and comparing against existing methods on three representative test problems. In each case, we use basis functions  $\{\phi_k\}_k$  corresponding to a degree- $p$  total-degree monomial basis,

$$(5.1) \quad \mathcal{P}_d^p := \{\phi_{\alpha}(\mathbf{x})\}_{|\alpha| \leq p}, \quad \phi_{\alpha}(\mathbf{x}) = \prod_{i=1}^d x_i^{\alpha_i}, \quad |\alpha| := \sum_{i=1}^d \alpha_i$$

where  $\alpha \in \mathbb{Z}_+^d$  is a multi-index over  $d$  nonnegative integers. In all our experiments we choose the basis  $\mathcal{P}_d^p$  with the smallest  $p$  containing the example differential equation.

**5.1. Test Problems.** Here we consider three common test problems the Duffing oscillator, Lorenz 63 attractor, and the Van der Pol Oscillator; see, e.g., [6, 9, 20]. We focus on these low-dimensional problems where we can perform Monte Carlo tests to evaluate performance over multiple realizations of noise. Unless otherwise mentioned, we use the sample rate  $\delta = 10^{-2}$ . To generate measurements  $\vec{\mathbf{y}}$ , we first evolve the corresponding differential equation using SciPy's `solve_ivp` with the DOP853 integrator to generate  $\vec{\mathbf{y}}$ . Then to generate noisy measurements, we sample  $\vec{\mathbf{n}} \sim \mathcal{N}(\vec{\mathbf{0}}, \vec{\Sigma})$  and form  $\vec{\mathbf{y}} = \vec{\mathbf{x}} + \vec{\mathbf{n}}$ .

**5.1.1. Duffing Oscillator.** The Duffing oscillator models a nonlinear pendulum; here we considered a damped variant where

$$(5.2) \quad \begin{cases} \dot{x}_1 = x_2, & x_1(0) = -2, \\ \dot{x}_2 = -0.1x_2 - x_1 - 5x_1^3, & x_2(0) = -2. \end{cases}$$

In our experiments, we typically use  $m = 1000$  measurements of this system.

**5.1.2. Lorenz 63 Attractor.** The Lorenz 63 attractor is a chaotic system developed initially from models of atmospheric convection:

$$(5.3) \quad \begin{cases} \dot{x}_1 = 10(x_2 - x_1), & x_1(0) = -8, \\ \dot{x}_2 = x_1(28 - x_3) - x_2, & x_2(0) = 7, \\ \dot{x}_3 = x_1x_2 - \frac{8}{3}x_3, & x_3(0) = -28. \end{cases}$$

In our experiments, we typically use  $m = 2000$  measurements of this system.

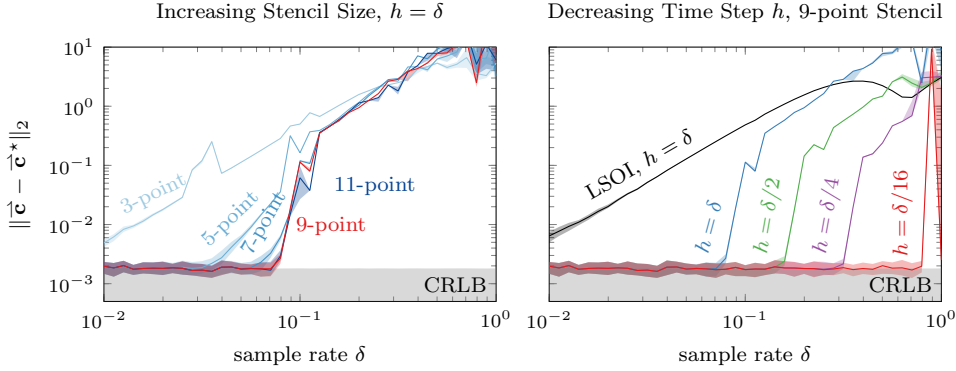


FIG. 5.1. Decreasing the discretization error in the ODE constraint of SIDDS improves the ability to recover a dynamical system. We use two techniques: increasing the order of the derivative approximation (left) and decreasing the time-step (right). In this example we collect  $m = 1000$  measurements of the Van der Pol system starting from a point on its limit cycle, adding i.i.d. normal noise with standard deviation  $\sigma = 10^{-3}$ . We estimate  $\vec{c}$  using SIDDS with  $\vec{M} = \vec{I}$  on the left and an expanded  $\vec{M}^\dagger$  on the right. The shaded region encloses the range between the 25th to 75th percentiles from 100 trials; the solid line indicates the median. The gray shaded region indicates the lower bound on performance given by the Cramér-Rao Lower Bound (CRLB).

**5.1.3. Van der Pol Oscillator.** The Van der Pol oscillator is a nonlinear ODE with a non-trivial limit cycle

$$(5.4) \quad \begin{cases} \dot{x}_1 = x_2, & x_1(0) = 0, \\ \dot{x}_2 = 2x_2(1 - x_1^2) - x_1, & x_2(0) = 1. \end{cases}$$

In our experiments, we typically use  $m = 1000$  measurements of this system.

**5.2. Tuning ODE Integration.** Both SIDDS and LSOI introduce a bias in the coefficients  $\vec{c}$  proportional to the discretization error of the ODE. With SIDDS though we have two techniques we can employ to reduce this error: increasing the accuracy of the derivative approximation by using a larger finite difference stencil and decreasing the time step in the ODE constraint. Both techniques are illustrated in Figure 5.1 with the Van der Pol example where we decrease the sample rate to increase the discretization error. In this example we also initialize the system at a point on its limit cycle so that the CRLB remains approximately constant irrespective of sample rate.

Decreasing discretization error by using a higher order finite difference stencil is successful, but yields diminishing returns beyond a 9-point stencil as this example illustrates. Moreover, larger stencils increase computational cost because increasing the stencil width increases the bandwidth of  $\vec{L}$  (4.11) and consequently the cost of its LU factorization. We use this 9-point stencil in all remaining experiments.

Another way to decrease the discretization error is to decrease the time step. With SIDDS we can set the ODE integration time step  $h$  to be any positive integer fraction of the sample rate  $\delta$ . For example, if we want to integrate with time step  $h = \delta/2$ , we introduce a zero vector between every measurement  $\mathbf{y}_j$  and a corresponding zero block in the weight matrix  $\vec{M}$ ; assuming  $\vec{M} = \mathbf{I}$ ,

$$(5.5) \quad \vec{\mathbf{y}}^\dagger = [\mathbf{y}_1^\top \quad \mathbf{0} \quad \mathbf{y}_2^\top \quad \mathbf{0} \quad \cdots \quad \mathbf{y}_m^\top]^\top, \quad \vec{\mathbf{M}}^\dagger = \text{diag}(\mathbf{I}_d, \mathbf{0}_d, \mathbf{I}_d, \mathbf{0}_d, \cdots, \mathbf{I}_d),$$

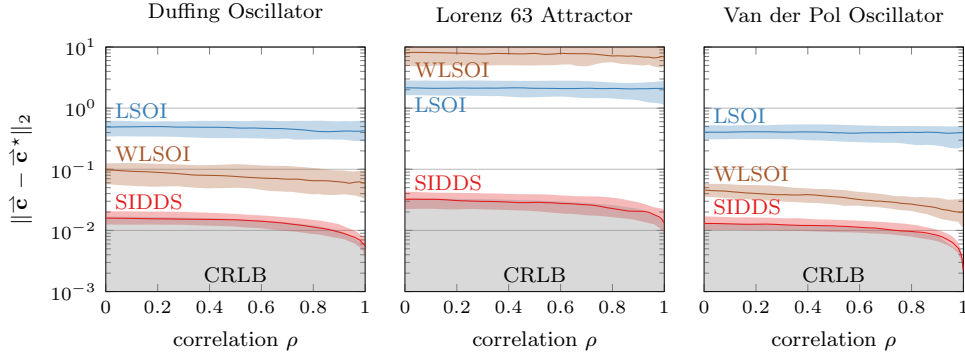


FIG. 5.2. *SIDDS* obtains the lower bound when taking  $\vec{\mathbf{M}} = \vec{\Sigma}^{-1}$  for correlated measurements described by (5.6) with  $\sigma = 10^{-2}$ . *WLSOI* refers to the weighted variant of *LSOI* described in (5.7).

where  $\mathbf{I}_d$  and  $\mathbf{0}_d$  are the  $d \times d$  identity and zeros matrices. This new  $\vec{\mathbf{y}}^\dagger$  has (effectively) half the sample rate,  $\delta^\dagger = h = \delta/2$ , and the zeros in  $\vec{\mathbf{M}}^\dagger$  ensure the values added between measurements do not affect the objective. As Figure 5.1 shows, solving *SIDDS* with these expanded quantities  $\vec{\mathbf{y}}^\dagger$  and  $\vec{\mathbf{M}}^\dagger$  allows the accurate identification even with slow sample rates  $\delta$ —something not possible with *LSOI*. Although useful when sample rate is slow relative to the dynamics, decreasing the time step substantially increases the cost solving the *SIDDS* problem. As our remaining examples are not in this regime, we use the same time step as the sample rate ( $h = \delta$ ) in the rest of our experiments.

**5.3. Correlated Noise.** With *SIDDS*, we can also incorporate knowledge of noise correlation. Suppose that noise  $\mathbf{n}_j$  at time  $j$  is correlated between coordinates with correlation  $\rho \in [0, 1)$ :

$$(5.6) \quad \mathbf{n}_j \sim \mathcal{N}\left(\mathbf{0}, \sigma^2 \begin{bmatrix} 1 & \rho \\ \rho & 1 \end{bmatrix}\right), \text{ if } \mathbf{n}_j \in \mathbb{R}^2; \quad \mathbf{n}_j \sim \mathcal{N}\left(\mathbf{0}, \sigma^2 \begin{bmatrix} 1 & \rho & 0 \\ \rho & 1 & 0 \\ 0 & 0 & 1 \end{bmatrix}\right), \text{ if } \mathbf{n}_j \in \mathbb{R}^3.$$

Then  $\vec{\mathbf{n}} \sim \mathcal{N}(\vec{\mathbf{0}}, \vec{\Sigma})$  where  $\vec{\Sigma}$  is a block diagonal matrix consisting of  $m$  repetitions of the block above. Taking the weight  $\vec{\mathbf{M}} = \vec{\Sigma}^{-1}$  in *SIDDS*, we obtain near optimal estimates as shown in Figure 5.2.

Could we incorporate knowledge that noise has the distribution  $\vec{\mathbf{n}} \in \mathcal{N}(\vec{\mathbf{0}}, \vec{\Sigma})$  into *LSOI*? We are not aware of any existing work that does, but we can use a weighted *LSOI*; i.e., for some  $\vec{\Gamma}$ , solving

$$(5.7) \quad \min_{\vec{\mathbf{c}}} \|\vec{\Gamma}[\vec{\mathbf{D}}\vec{\mathbf{y}} - \vec{\Phi}(\vec{\mathbf{y}})\vec{\mathbf{c}}]\|_2^2.$$

In a linear estimation problem  $\min_{\vec{\mathbf{c}}} \|\vec{\Gamma}[\vec{\mathbf{y}} - \vec{\mathbf{A}}\vec{\mathbf{c}}]\|_2^2$  we choose  $\vec{\Gamma} = \vec{\Sigma}^{-1/2}$  so that the residual is i.i.d. normally distributed (this is sometimes called *whitening*). Similarly, for *LSOI* linearizing around the true solution yields  $\vec{\Gamma} = \vec{\Sigma}^{-1/2}[\vec{\mathbf{D}} - \nabla\vec{\Phi}(\vec{\mathbf{x}})\vec{\mathbf{x}}_2\vec{\mathbf{c}}^*]^+$ . As seen in Figure 5.2 this approach can sometimes yield improvements over unweighted *LSOI*, but the ill-conditioning of  $\vec{\Gamma}$  limits the utility of this approach. If we use a rank-truncated pseudoinverse we can recover estimates that nearly obtain the CRLB at the cost of an  $\mathcal{O}((md)^3)$  operation SVD; this infeasible for large problems. Ill-conditioning can be avoided by reformulating weighted *LSOI* as a constrained

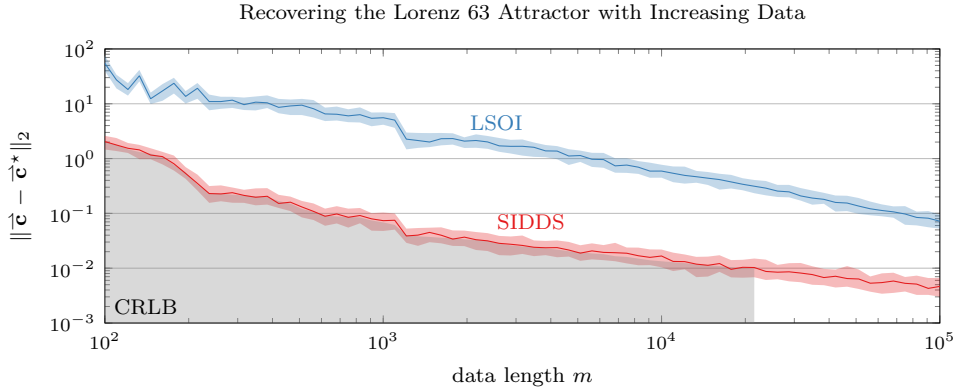


FIG. 5.3. *SIDDS* enables the accurate recovery of dynamical systems with less data than *LSOI*. This example considers the Lorenz 63 attractor with sample rate  $\delta = 10^{-2}$  and additive *i.i.d.* normally distributed noise with standard deviation  $\sigma = 10^{-2}$ , using  $\bar{\mathbf{M}} = \mathbf{I}$  in *SIDDS*. Numerics limit the ability to compute the *CRLB* for large  $m$ .

optimization problem,

$$(5.8) \quad \begin{aligned} \min_{\bar{\mathbf{c}}, \bar{\mathbf{r}}} \quad & \|\bar{\Sigma}^{-1/2} \bar{\mathbf{r}}\|_2 \\ \text{s.t.} \quad & [\bar{\mathbf{D}} - \nabla \bar{\Phi}(\bar{\mathbf{x}}) \bar{\Sigma}_2 \bar{\mathbf{c}}^*] \bar{\mathbf{r}} = \bar{\mathbf{D}} \bar{\mathbf{y}} - \bar{\Phi}(\bar{\mathbf{y}}) \bar{\mathbf{c}}; \end{aligned}$$

however, at this point we have reinvented *SIDDS*, albeit using a different set of variables and a linearized constraint around the true values  $\bar{\mathbf{c}}^*$  and  $\bar{\mathbf{x}}$ .

**5.4. Large Data.** The previous example showed that *SIDDS* recovers more accurate estimates than *LSOI*. Another interpretation of this result is that *SIDDS* obtains similarly accurate estimates using less data. Figure 5.3 illustrates this point by recovering the chaotic Lorenz 63 attractor with increasing amounts of data. We observe *SIDDS* obtains roughly the same accuracy as *LSOI* using ten times less data. This example also serves as a stress-test of *SIDDS*, illustrating that the algorithm scales to large scale problems while still approximately obtaining the *CRLB*.

**5.5. Comparing *SIDDS* to Other Algorithms.** As a final example, Figure 5.4 compares algorithms for estimating dynamical systems perform with increasing levels of noise. We separate these algorithms into two classes: those without a sparsity promoting constraint (*LSOI* and *SIDDS*) and those with a sparsity promoting constraint (*SINDy*+*STLS* [6, 12], Modified *SINDy* [20], and *SIDDS*+ $\ell_0$ ) since sparsity promotion allows for an improved recovery and lowers the *CRLB* as discussed in subsection 3.1.2. These experiments illustrate several key points. First, *SIDDS* and *SIDDS*+ $\ell_0$  approximately obtain the Cramér-Rao lower bound for small noise  $\sigma$ ; for large noise, these algorithms identify a local minimizer far away the true solution leading the estimates to detach from the lower bound. Second, while the denoising penalty introduced by *mSINDy* does improve estimates compared to *SINDy*+*STLS*, it does not obtain the lower bound. Third, *SIDDS*+ $\ell_0$  is able to correctly identify the sparsity structure for larger noise than *SINDy*+*STLS* and *mSINDy*.

**6. Discussion.** Here we have shown how to practically identify and denoise a dynamical system using *SIDDS* and how to incorporate sparsity promotion in *SIDDS*+ $\ell_0$ . This algorithm yields estimates obtaining the Cramér-Rao lower bound for small noise,

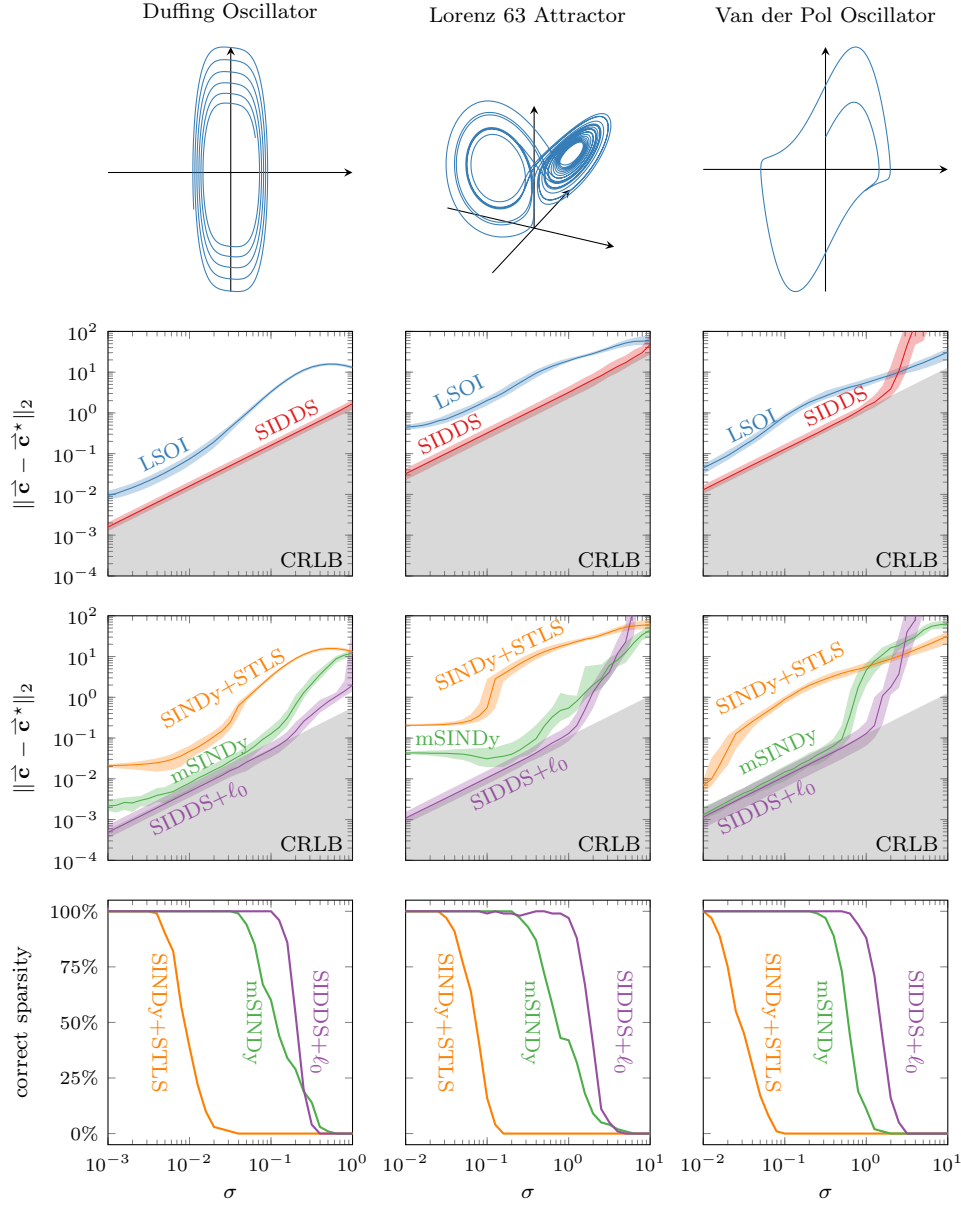


FIG. 5.4. Both the SIDDS and the sparsity promoting SIDDS+l<sub>0</sub> obtain better estimates than competing methods. For each test problem, we consider how each method performs as the standard deviation  $\sigma$  of the additive *i.i.d.* normally distributed noise increases. The second row considers unregularized algorithms: SIDDS (with  $\hat{\mathbf{M}} = \hat{\mathbf{I}}$ ) and LSQI. The third row considers sparsity promoting algorithms: SINDy using STLS as implemented in PySINDy [12, 22] (SINDy+STLS), Modified SINDy as implemented by [20] (mSINDy), and SIDDS+l<sub>0</sub> (with  $\hat{\mathbf{M}} = \hat{\mathbf{I}}$ ). The CRLB for this row is computed assuming the correct sparsity structure in  $\hat{\mathbf{c}}$  yielding a smaller lower bound than the preceding row as discussed in subsection 3.1.2. Here we use sample rate  $\delta = 10^{-2}$  and  $m$  of 1000, 2000, and 1000 for Duffing, Lorenz 63, and Van der Pol respectively. For SINDy+STLS we use the default parameters in PySINDy. For mSINDy we use parameters from [20]: truncation parameter  $\lambda$  of 0.05, 0.2, and 0.1 and ADAM steps per outer iteration of 5000, 15000, and 5000 respectively. For SIDDS+l<sub>0</sub>, we choose the penalty  $\alpha$  of 0.01, 0.5, and 1 respectively chosen via a coarse optimization to maximize the probability of recovering the correct sparsity structure with large noise.

outperforming existing algorithms. We anticipate there many possible avenues for improvement and extension of SIDDS; e.g., better initialization through smoothing techniques described in [10] and incorporating nonautonomous input as in [21].

## REFERENCES

- [1] N. ALGER, U. VILLA, T. BUI-THANH, AND O. GHATTAS, *A data scalable augmented Lagrangian KKT preconditioner for large-scale inverse problems*, SIAM J. Sci. Comput., 39 (2017), pp. A2365–A2393, <https://doi.org/10.1137/16m1084365>.
- [2] M. ASCH, M. BOCQUET, AND M. NODET, *Data Assimilation*, Society for Industrial and Applied Mathematics, Dec. 2016, <https://doi.org/10.1137/1.9781611974546>.
- [3] Z. BEN-HAIM AND Y. C. ELДАР, *On the constrained Cramér–Rao bound with a singular Fisher information matrix*, IEEE Signal Process. Lett., 16 (2009), pp. 453–456, <https://doi.org/10.1109/lsp.2009.2016831>.
- [4] Å. BJÖRCK, *Numerical Methods for Least Squares Problems*, SIAM, Philadelphia, PA, 1996.
- [5] T. BLUMENSATH AND M. E. DAVIES, *Iterative hard thresholding for compressed sensing*, Appl. Comput. Harmon. A., 27 (2009), pp. 265–274, <https://doi.org/10.1016/j.acha.2009.04.002>.
- [6] S. L. BRUNTON, J. L. PROCTOR, AND J. N. KUTZ, *Discovering governing equations from data by sparse identification of nonlinear dynamical systems*, Proc. Natl. Acad. Sci. USA, 113 (2016), pp. 3932–3937.
- [7] E. J. CANDÈS, M. B. WAKIN, AND S. P. BOYD, *Enforcing sparsity by reweighted  $\ell_1$  minimization*, J. Fourier Anal. Appl., 14 (2008), pp. 877–905, <https://doi.org/10.1007/s00041-008-9045-x>.
- [8] R. CHARTRAND AND W. YIN, *Iteratively reweighted algorithms for compressive sensing*, in 2008 IEEE International Conference on Acoustics, Speech and Signal Processing, IEEE, Mar. 2008, <https://doi.org/10.1109/icassp.2008.4518498>.
- [9] A. CORTIELLA, K.-C. PARK, AND A. DOOSTAN, *Sparse identification of nonlinear dynamical systems via reweighted  $\ell_1$ -regularized least squares*, Comput. Method. Appl. M., 376 (2021), p. 113620, <https://doi.org/10.1016/j.cma.2020.113620>.
- [10] A. CORTIELLA, K.-C. PARK, AND A. DOOSTAN, *A priori denoising strategies for sparse identification of nonlinear dynamical systems: A comparative study*, 2022, <https://arxiv.org/abs/2201.12683v1>.
- [11] I. DAUBECHIES, R. DEVORE, M. FORNASIER, AND C. S. GÜNTÜRK, *Iteratively reweighted least squares minimization for sparse recovery*, Comm. Pure Appl. Math., 63 (2010), pp. 1–38, <https://doi.org/10.1002/cpa.20303>.
- [12] B. DE SILVA, K. CHAMPION, M. QUADE, J.-C. LOISEAU, J. KUTZ, AND S. BRUNTON, *PySINDy: A Python package for the sparse identification of nonlinear dynamical systems from data*, JOSS, 5 (2020), p. 2104, <https://doi.org/10.21105/joss.02104>.
- [13] J. W. DEMMEL, S. C. EISENSTAT, J. R. GILBERT, X. S. LI, AND J. W. H. LIU, *A supernodal approach to sparse partial pivoting*, SIAM J. Matrix Anal. & Appl., 20 (1999), pp. 720–755, <https://doi.org/10.1137/s0895479895291765>.
- [14] G. H. GOLUB AND V. PEREYRA, *The differentiation of pseudo-inverses and nonlinear least squares problems whose variables separate*, SIAM J. Numer. Anal., 10 (1973), pp. 413–432, <https://doi.org/10.1137/0710036>.
- [15] G. H. GOLUB AND C. F. VAN LOAN, *Matrix Computations*, Johns Hopkins University Press, Baltimore, MD, fourth ed., 2013.
- [16] E. HABER AND U. M. ASCHER, *Preconditioned all-at-once methods for large, sparse parameter estimation problems*, Inverse Probl., 17 (2001), pp. 1847–1864, <https://doi.org/10.1088/0266-5611/17/6/319>.
- [17] E. HABER, U. M. ASCHER, AND D. OLDENBURG, *On optimization techniques for solving nonlinear inverse problems*, Inverse Probl., 16 (2000), pp. 1263–1280, <https://doi.org/10.1088/0266-5611/16/5/309>.
- [18] M. HEINKENSCHLOSS, *Numerical solution of implicitly constrained optimization problems*, Tech. Report TR08-05, Rice University, 2013, <https://hdl.handle.net/1911/102087>.
- [19] R. A. HORN AND C. R. JOHNSON, *Matrix Analysis*, Cambridge University Press, second ed., 2012, <https://doi.org/10.1017/cbo9781139020411>.
- [20] K. KAHEMAN, S. L. BRUNTON, AND J. N. KUTZ, *Automatic differentiation to simultaneously identify nonlinear dynamics and extract noise probability distributions from data*, 2020, <https://arxiv.org/abs/2009.08810v2>.
- [21] E. KAISER, J. KUTZ, AND S. BRUNTON, *Sparse identification of nonlinear dynamics for model predictive control in the low-data limit*, Proc. R. Soc. A., 474 (2018), p. 20180335, <https://doi.org/10.1098/rspa.2018.0335>.



- doi.org/10.1098/rspa.2018.0335, <https://doi.org/10.1098/rspa.2018.0335>.
- [22] A. A. KAPTANOGLU, B. M. DE SILVA, U. FASEL, K. KAHAMAN, A. J. GOLDSCHMIDT, J. L. CALLAHAM, C. B. DELAHUNT, Z. G. NICOLAOU, K. CHAMPION, J.-C. LOISEAU, J. N. KUTZ, AND S. L. BRUNTON, *PySINDy: A comprehensive Python package for robust sparse system identification*, arXiv preprint arXiv:2111.08481, (2021).
  - [23] T. G. KOLDA AND B. W. BADER, *Tensor decompositions and applications*, SIAM Rev., 51 (2009), pp. 455–500, <https://doi.org/10.1137/07070111X>.
  - [24] M.-J. LAI, Y. XU, AND W. YIN, *Improved iteratively reweighted least squares for unconstrained smoothed  $\ell_q$  minimization*, SIAM J. Numer. Anal., 51 (2013), pp. 927–957, <https://doi.org/10.1137/110840364>.
  - [25] X. LIU AND Y. YUAN, *A sequential quadratic programming method without a penalty function or a filter for nonlinear equality constrained optimization*, SIAM J. Optim., 21 (2011), pp. 545–571, <https://doi.org/10.1137/080739884>.
  - [26] B. PEHERSTOFER AND K. WILLCOX, *Data-driven operator inference for nonintrusive projection-based model reduction*, Comput. Methods Appl. Mech. Engrg., 306 (2016), pp. 196–215, <https://doi.org/10.1016/j.cma.2016.03.025>.
  - [27] S. H. RUDY, J. N. KUTZ, AND S. L. BRUNTON, *Deep learning of dynamics and signal-noise decomposition with time-stepping constraints*, J. Comput. Phys., 396 (2019), pp. 483–506, <https://doi.org/10.1016/j.jcp.2019.06.056>.
  - [28] G. A. F. SEBER AND C. J. WILD, *Nonlinear Regression*, Wiley-Interscience, 1989.
  - [29] F. SUN, Y. LIU, AND H. SUN, *Physics-informed spline learning for nonlinear dynamics discovery*, in Proceedings of the Thirtieth International Joint Conference on Artificial Intelligence, International Joint Conferences on Artificial Intelligence Organization, Aug. 2021, <https://doi.org/10.24963/ijcai.2021/283>.
  - [30] G. TRAN AND R. WARD, *Exact recovery of chaotic systems from highly corrupted data*, Multi-scale Model. Simul., 15 (2017), pp. 1108–1129, <https://doi.org/10.1137/16m1086637>.
  - [31] S. J. WRIGHT, *An algorithm for degenerate nonlinear programming with rapid local convergence*, SIAM J. Optim., 15 (2005), pp. 673–696, <https://doi.org/10.1137/030601235>.
  - [32] K. WU AND D. XIU, *Numerical aspects for approximating governing equations using data*, J. Comput. Phys., 384 (2019), pp. 200–221, <https://doi.org/10.1016/j.jcp.2019.01.030>, <https://doi.org/10.1016/j.jcp.2019.01.030>.